Missouri S&T Library and Learning Resources

Scholars' Mine

Masters Theses

Student Theses and Dissertations

1972

Design of a torsional vibration machine

Prafulchandra Pragjibhai Desai

Follow this and additional works at: https://scholarsmine.mst.edu/masters_theses

 Part of the Mechanical Engineering Commons

Department:

Recommended Citation

Desai, Prafulchandra Pragjibhai, "Design of a torsional vibration machine" (1972). *Masters Theses*. 5112.
https://scholarsmine.mst.edu/masters_theses/5112

This thesis is brought to you by Scholars' Mine, a service of the Missouri S&T Library and Learning Resources. This work is protected by U. S. Copyright Law. Unauthorized use including reproduction for redistribution requires the permission of the copyright holder. For more information, please contact scholarsmine@mst.edu.

DESIGN OF A TORSIONAL VIBRATION MACHINE

BY

PRAFULCHANDRA PRAGJIBHAI DESAI, 1945

A THESIS

Presented to the Faculty of the Graduate School of the

UNIVERSITY OF MISSOURI-ROLLA

In Partial Fulfillment of the Requirements for the Degree

MASTER OF SCIENCE IN MECHANICAL ENGINEERING

1972

Approved by

R D Rocke (Advisor) Wm L Gatley

Edward F Hornsey

ABSTRACT

In this thesis the design of the major components of a torsional vibration machine is presented. The machine is a torsional vibration actuator which will deliver a mean output angular velocity with a superimposed harmonic component. This type of motion can be used to study the torsional vibration characteristics of models representing crankshafts, gear trains, torsional dampers, and other systems.

The primary machine elements of the actuator are a power source, flywheel, and a Hooke's joint. The power source consists of a D.C. shunt motor and a drive transmission using 3 V-belts. Through the use of a Hooke's joint, approximate sinusoidal angular velocity variations superimposed upon a mean angular velocity are generated at the output shaft. The effects of the variations in the output shaft speed upon that of the input shaft are minimized by the use of a flywheel. This is essential to generate nearly sinusoidal variations in the output shaft speed. The flywheel design is such that its inertia can be changed in steps by addition or subtraction of segments to a disc flywheel.

Specimens to be tested with the motion generated are rigidly connected to the output shaft of the Hooke's joint. The frequency of the sinusoidal input motion to the

specimen is varied by changing the input shaft speed of the Hooke's joint. By using a D.C. shunt motor with field control equipment, the input shaft speed can be adjusted to any desired speed within the range 370-1000 RPM. As the frequency of variation of the output shaft is nearly a second harmonic of the input shaft speed, the corresponding range of frequency of variation at the specimen is 12-33 cps. The amplitude of variation at the specimen is established by changing the angle between the input and output shafts of the Hooke's joint. This angle is limited to $\pm 20^{\circ}$, as beyond this angle the variations in the output shaft velocity do not closely approximate sinusoidal conditions. The amplitude of the mean output velocity is controlled by the input velocity.

The machine vibrations within the actuator system are isolated from the supporting structure by placing the machine on isomode vibration pads. The isolation system is designed such that the ratio of the lowest forcing frequency during testing and the fundamental frequency of the rubber pad-machine system is greater than 1.4, i.e., the transmissibility is less than one.

ACKNOWLEDGEMENTS

The author wishes to express his sincere thanks to Dr. Richard D. Rocke for his encouragement, direction and assistance throughout the course of this thesis. The author also wishes to thank Dr. William S. Gatley for his valuable suggestions.

The author is thankful to Mrs. Connie Hendrix and Mrs. Sandra Davis for typing the manuscript.

TABLE OF CONTENTS

TABLE OF CONTENTS (con't)

LIST OF ILLUSTRATIONS

LIST OF ILLUSTRATIONS (con't)

LIST OF ILLUSTRATIONS (con't)

LIST OF TABLES

CHAPTER I
INTRODUCTION

The analysis of vibration problems has become more important in Mechanical Design as machine elements become larger and their relative velocities become greater. Many problems of practical significance, such as balancing of machines, the torsional vibration of shafts and geared systems, the vibrations of turbine blades and discs, the whirling of rotating shafts and other similar problems can be thoroughly understood only by including the theory of vibration. To validate theoretical investigations, experimental means are always necessary. For rotational problems which are nonlinear or which in other ways do not allow for the superposition of a mean plus a periodically varying rotation, a rotational source of motion is required for experimental measurements.

The objective herein is to consider the design of a machine which provides a mean angular velocity upon which a sinusoidal variation can be superimposed. This machine should duplicate a realistic environment such that torsional vibration characteristics can be thoroughly investigated for gear trains, crankshafts, torsional dampers etc. This machine should have particular application to nonlinear problems; for example, an impact damper, a shaft coupling which uses rubber; which demand the presence of complete rotational motion.

Although extensive work has been done in analysis of linear torsional vibration, few devices that simulate the conditions causing torsional vibrations have been made. Yada[1] has devised an alternating torque generator incorporating planetary gears with unbalanced masses. It is so constructed that the amplitude and the frequency of the alternating torque can be varied independently of both the rotation of the load and the motor. Yada has analyzed this device both theoretically and experimentally. Experiments were made with a friction type stepless speed variator to measure angular velocity of the system and also with an elastic coupling to determine the effect of the radial clearance between the rubber bushes and the holes in the coupling on the amplitude of vibration. The results, in the latter case, show that the amplitude becomes severe as the generator torque amplitude increases. The experiments by Yada were limited to 20 cps and 80 lb-in torque amplitude because of the natural frequency of the system and the capacity of the torque transducer. Yada concludes that this type of equipment could be improved to have higher performance capabilities in frequency and torque amplitude.

Ashar[2] has made a feasibility study of a torsional vibration actuator incorporating a Hooke's joint. He has found that a single Hooke's joint can be used to generate a sinusoidally varying angular motion superimposed on a constant angular motion. This is the type of motion of interest. The design objective of this thesis is to implement a

design which uses a Hooke's joint.

A. Design Criteria

Ashar has analyzed a torsional vibration actuator theoretically, having developed the equations of motion for a particular machine and obtained solutions numerically. From the study of his work, it is evident that a torsional vibration testing machine should satisfy the following criteria:

1) It should be very rigid in comparison to specimens being excited by the machine such that a negligible amount of motion from machine flexibility is coupled to the specimen. Each element or member of the machine should have adequate strength. Also, it should be economical to manufacture.

2) It should generate a sinusoidally varying angular velocity superimposed upon a mean angular velocity, which would simulate the conditions causing torsional vibrations.

3) It should have the capability for testing at different frequencies as well as different amplitudes of vibration.

B. Description of Operation

From Ashar's feasibility study it was found that a single Hooke's joint can be used to generate an angular velocity composed of a mean velocity with a superimposed component which can be controlled to be approximately sinusoidal. Hence, a Torsional Vibration Actuator would essentially consist of a power source, a Hooke's joint

and a specimen rigidly connected to the driven shaft of the Hooke's joint. The power source may consist of an electric motor plus either a gear drive, a belt drive, or an adjustable speed drive. The input side, called the drive assembly would consist of the power source, a flywheel, the drive shaft of the Hooke's joint, ball or roller bearings to support the drive shaft, bearing supports, etc. The output side, called the driven assembly, would consist of the driven shaft of the Hooke's joint, a specimen, bearings and bearing support structures, etc. It would also be essential to hinge either the drive assembly or the driven assembly, the center of the hinge being exactly below the center of the Hooke's joint, to facilitate testing at different angles of the Hooke's joint.

For a constant drive speed, the frequency of variation of the driven speed is nearly a second harmonic of the drive speed when the input and output sides of the Hooke's joint are not in a straight line. Hence, for different drive speeds the frequency of variation of the driven speed would be different. The amplitude of variation is established by changing the Hooke's joint angle. The Hooke's joint angle should be limited to $\pm 20^{\circ}$, as beyond this angle the variations in the output shaft velocity do not closely approximate sinusoidal conditions.

By using a flywheel in the drive side, the effects of variations in the driven shaft speed upon the drive shaft

speed are minimized and a nearly constant drive shaft speed is maintained. This is essential to obtain variations close to sinusoidal in the driven shaft speed.

CHAPTER II
DRIVE ASSEMBLY

The design of the Torsional Vibration Testing Machine is separated into two main subassemblies, i.e. the drive assembly and the driven assembly. The drive assembly is shown in Fig. 2.1 and includes a D.C. shunt motor, v-belt drive transmission, flywheel, bearings, and supporting structure. An assembly drawing and details of each element or member of the machine are given in Appendix A.

A. Design Criteria

The criteria pertinent to the design of the drive subassembly are: to obtain the kinematic motion desired; to obtain structural rigidity such that a negligible amount of motion from driver flexibility is coupled to the test specimen. Hence, the members should be designed so that they have small deflections. Since the frequency of vibration is inversely proportional to the square root of the deflection, the smaller the deflection, the higher the natural frequency. It is a general rule of design for vibration fixtures to design the fixture such that its fundamental natural frequency is four to five times higher than the highest frequency of testing. For the machine in consideration it is contemplated that testing may be done at rotational speeds of approximately 300 to 1500 RPM which correspond to forcing frequencies of 12 to

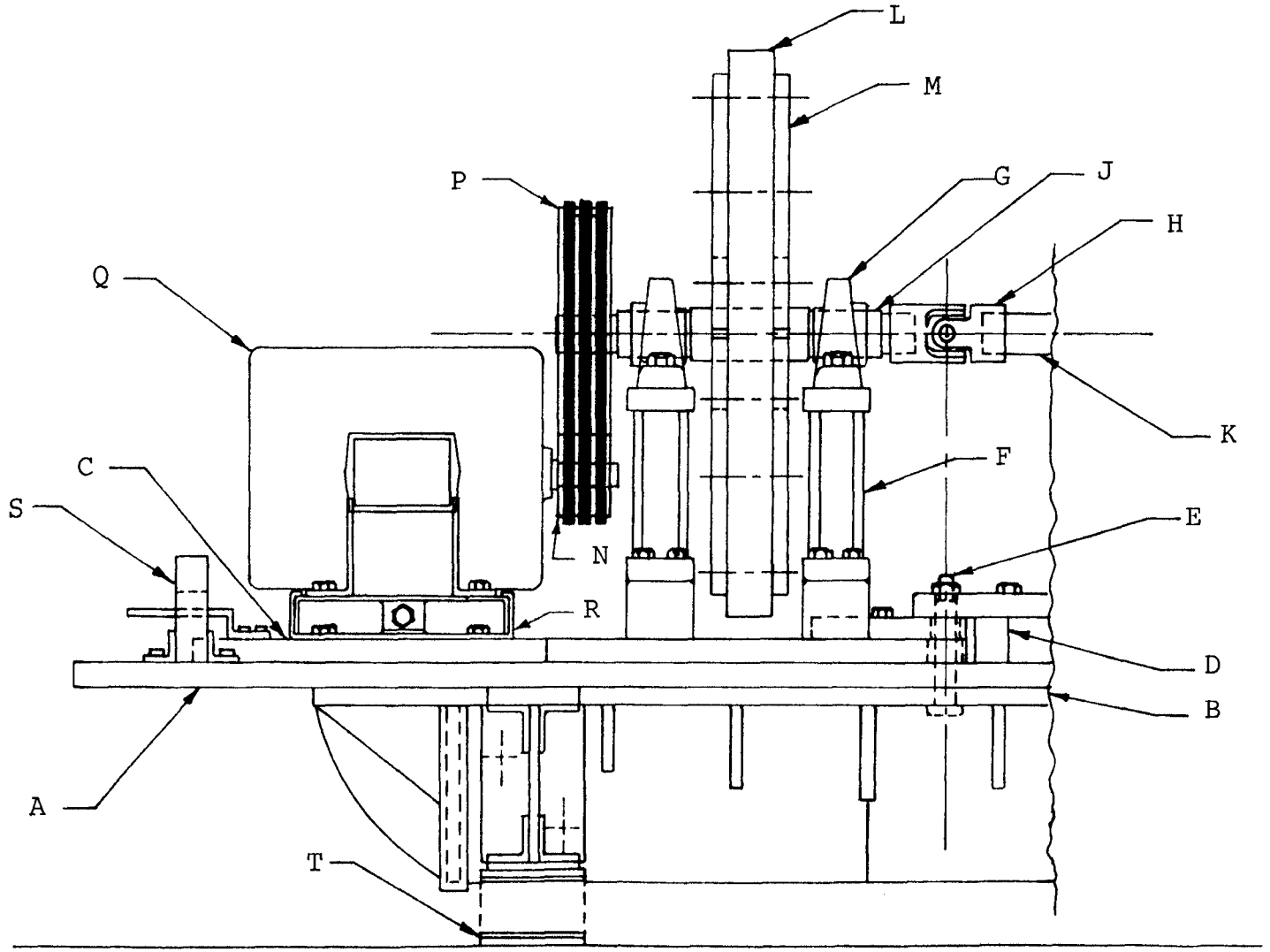

Fig. 2.1. Elevation View of the Drive Side

In Fig. 2.1,

A	Surface Plate Structure
B	Base Plate
C	Drive Plate
D	Pivot Assembly
E	Pivot Pin
F	Drive Shaft Bearing Support
G	Drive Shaft Bearing
H	Hooke's Joint
J	Drive Shaft
K	Driven Shaft
L	Flywheel
M	Flywheel Segment
N	Small Sheave
P	Large Sheave
Q	D.C. Motor
R	Motor Base
S	Mechanism to Change the Hooke's Joint Angle
T	Machine Mounting

50 cps at the output shaft of the machine. Hence, the subassemblies of the machine should all have resonant frequencies in excess of the range of 200 to 250 cps.

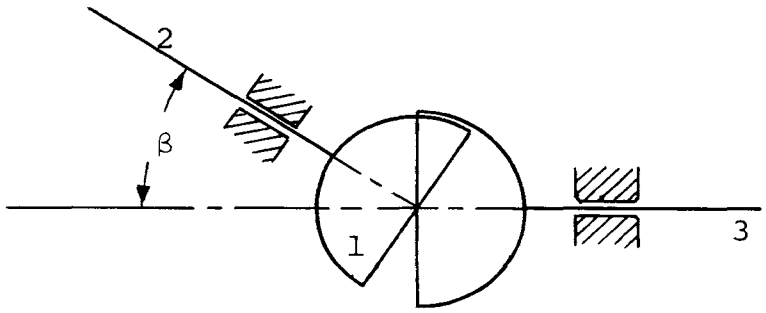

Fig. 2.2 Hooke's Joint

A sketch of a Hooke's joint is given in Fig. 2.2. In this figure, link 2 is the drive shaft and link 3 is the driven shaft. Link 1 is the cross piece that connects the two yokes. Equation (2.1) gives the relationship between ω_3, the angular velocity of the driven shaft and ω_2, the angular velocity of the drive shaft of a Hooke's joint.

$$\omega_3 = \left[\frac{\cos\beta}{1-\sin^2\beta\sin^2\theta}\right]\omega_2 \qquad (2.1)$$

where:

θ = Angular displacement of the drive shaft

β = Included angle between the shafts

Equation (2.1) can also be approximated in the form given by Eq. (2.2). The constants, c_5 and c_6, depend on the Hooke's joint angle β. For $\beta = 10^{\circ}$ and 20°, Eq. (2.2) reduces to Eq. (2.3) and (2.4), respectively.

$$\frac{\omega_3}{\omega_2} = \left[\frac{c_5}{c_6} - \frac{c_5}{c_6^2}\cos 2\theta + \frac{\frac{c_5}{c_6^2}\cos^2 2\theta}{c_6 + \cos 2\theta}\right] \tag{2.2}$$

$$\frac{\omega_3}{\omega_2} = \left[0.999 - 0.01533 \cos 2\theta + \frac{0.01533 \cos^2 2\theta}{65.225 + \cos 2\theta}\right] \tag{2.3}$$

$$\frac{\omega_3}{\omega_2} = \left[0.9981 - 0.0620 \cos 2\theta + \frac{0.06202 \cos^2 2\theta}{16.09 + \cos 2\theta}\right] \tag{2.4}$$

From Eq. (2.2) it can be noted that, for constant ω_2 the variation in the driven shaft velocity ω_3 is periodic in nature, approximately sinusoidal with two cyclic changes for one complete revolution of the drive shaft. In other-words, the frequency of variation of ω_3 is nearly a second harmonic of ω_2. Also, the ordinates, i.e., the values of ω_3/ω_2 measured from the datum $\omega_3/\omega_2 = 1$, at $\theta = 90^{\circ}$ and at $\theta = 180^{\circ}$ are not exactly equal, indicating a departure from pure sinusoidal motion. For $\beta = 10^{\circ}$ and 20°, the values of ω_3/ω_2 at $\theta = 90^{\circ}$ and 180° are represented by Eqs. (2.5) through (2.8), as indicated therein.

$$\omega_3/\omega_2 \ (\beta=10^\circ, \ \theta=90^\circ)=[0.999+0.01533+0.000238] \qquad (2.5)$$

$$\omega_3/\omega_2 \ (\beta=10^\circ, \ \theta=180^\circ)=[0.999-0.01533+0.000231] \qquad (2.6)$$

$$\omega_3/\omega_2 \ (\beta=20^\circ, \ \theta=90^\circ)=[0.9981+0.0602+0.00411] \qquad (2.7)$$

$$\omega_3/\omega_2 \ (\beta=20^\circ, \ \theta=180^\circ)=[0.9981-0.06202+0.00363] \qquad (2.8)$$

From these equations, it is noted that the amplitude of variation at the driven shaft depends on the Hooke's joint angle β. Both the amplitude and the deviations from pure sinusoidal motion increase as β increases. To limit the deviations from pure sinusoidal motion increase as β increases. To limit the deviations from pure sinusoidal motion, the Hooke's joint angle β must be limited to a certain maximum value. Limiting β to $\pm 20^\circ$ or less keeps the error level below ten percent where the error is defined by:

$$\% \text{ Error} = \frac{\text{Ordinate}(\theta = 90) - \text{Ordinate}(\theta = 180)}{\text{Average Ordinate}} \times 100 \qquad (2.9)$$

where an ordinate represents the value of ω_3/ω_2 measured from the datum $\omega_3/\omega_2 = 1$.

To determine torsional vibration characteristics, specimens should be tested over a range of forcing frequencies. Therefore, the power source should be such that the drive shaft speed can be adjusted to different values. Also, to facilitate testing at different angles of the Hooke's joint, i.e., at different amplitudes of vibration,

either the drive assembly or driven assembly should be hinged, the center of the hinge being exactly below the center of the Hooke's joint. It is preferable to hinge the drive assembly because:

1. The drive shaft has a nearly constant angular velocity.
2. Higher amplitude vibrations occur in the specimen, therefore, the supporting structure for the specimen should be rigidly connected to the base of the machine.
3. Due to instrumentation, most of which would be on the driven side, it may not be desirable to move the driven assembly.

The flywheel minimizes the effect of the inertia torque transferred from the driven side to the drive side. Thus, it helps in maintaining a nearly constant drive shaft speed which is desirable to obtain a nearly sinusoidal variation in the driven shaft speed. Thus, large test items will require a larger flywheel inertia to retain the same level of deviation in the driven shaft speed. Also, one may want to examine the effects of deviation from sinusoidal motion on the specimen motion. Considering these aspects a flywheel whose mass moment of inertia can be changed, should be designed.

Due to the nature of the machine, rocking and torsional vibrations are expected in the drive and driven assemblies. Therefore, the assemblies should be analyzed and designed to insure minimal structural response, i.e., the principal mode frequencies of the machine should be in

excess of the excitation frequencies used in testing.

Design experience has shown that elements designed on the basis of minimal deflections generally result in relatively small stresses. Therefore, stress analyses may not be required for all of the members of the machine. However, stresses should be calculated in appropriate members to check that they are within safe limits.

B. Power Source

The power source selected consists of a D.C. shunt motor and a multiple v-belt drive transmission whose output/input ratio can be changed by changing pulley ratios. A transmission ratio of 3.11 and a D.C. shunt motor of 1.5 H.P. with appropriate field control equipment were selected for satisfactory operation using test specimens with inertias up to 0.314 lb-in-sec^2. This system enables one to adjust the speed of the drive shaft, in this instance, to any particular speed between and including 377.5 RPM to 964 RPM. The corresponding frequency of angular velocity variation at the specimen would be 12-32 cps.

1. Motor

It has been shown in Eq. (2.1) that the nature of the driven shaft velocity depends on the characteristic of the drive shaft velocity. If ω_2 is nearly constant, the variations in the driven shaft velocity ω_3 are nearly sinusoidal. Because of this a D.C. shunt motor which

exhibits a good speed regulation characteristic is selected as a prime mover. In the shunt wound motor the strength of the field is not affected appreciably by change in the load, so that a fairly constant speed is obtainable. The speed of the motor can be adjusted to different values by means of a field control. Thus, a D.C. shunt motor with an appropriate field control equipment provides the facility for testing at different frequencies of variation at the specimen.

The motor supplies power to overcome the friction and the inertia torque exerted by the driven parts. As the driven shaft has a periodic acceleration, which is nearly sinusoidal, a torque from the driven side is exerted on the flywheel. This causes a change in the flywheel speed, perturbing it from a constant value. Because of the flywheel inertia the amplitude of variation in the drive shaft speed is much smaller than that for the driven shaft[2]. When the steady state conditions are reached, the motor has to supply the power to accelerate the driven parts from the mean speed to maximum speed. The approximate horse power of the motor can be calculated by using the average value of sinusoidally varying load torque.

2. V-Belt Drive

The factors considered in selecting the method of transmission of power were the center distance between the motor and the drive shaft and cost. For a short distance

either a v-belt drive or a gear drive could be used. Cost considerations lead to the selection of a v-belt drive.

(a) Procedure of Selection

Given Conditions:

Speed range of the driven unit - 370 to 1000 RPM.

Speed range of the drive unit - 1150 to 3000 RPM. (D.C. shunt motor)

Motor H.P. - 1.5

Desired transmission ratio - 3.0

From Table 15.7 of Ref. (3) an "A" section belt is selected as it permits the use of a smaller sheave. Taking the pitch diameter of the small sheave as 3.4 inches, the diameter of the large sheave is:

$$D = d\frac{n_1}{n_2} \qquad (2.10)$$

Where:

D = Diameter of the large sheave, in.

d = Diameter of the small sheave, in.

n_1 = RPM of the motor.

n_2 = RPM of the large sheave.

Substituting for d = 3.4 in., n_1 = 370 RPM, n_2 = 1150 RPM into Eq. (2.10), gives:

$$D = 3.4 \times \frac{1150}{370} = 10.2 \text{ in.}$$

A standard diameter of 10.6 inches is selected.

A center distance of 10.6 inches is tentatively selected. The angle of contact is given by:

$$\theta_c = \pi \pm 2 \sin^{-1}\left(\frac{D-d}{2c}\right) \qquad (2.11)$$

where

θ_c = Angle of contact, rad.

c = Center distance, in.

The angle of contact on the large sheave is:

$$\theta_{cL} = \pi + 2 \sin^{-1}\left(\frac{10.6-3.4}{2 \times 10.6}\right) = 3.8346 \text{ rad. or } 219.8^{\circ}$$

The angle of contact on the small sheave is:

$$\theta_{cs} = \pi - 2 \sin^{-1}\left(\frac{10.6-3.4}{2 \times 10.6}\right) = 2.4454 \text{ rad. or } 140.2^{\circ}$$

The length of the belt is given by:

$$L = \sqrt{4c^2-(D-d)^2} + 1/2[D\theta_{cL}+d\theta_{cs}] \qquad (2.12)$$

$$L = \sqrt{4x10.6^2-(10.6-3.4)^2} + 1/2[(10.6)(3.8346)+(3.4)$$

$$(2.4454)] = 44.35 \text{ in.}$$

An A42 belt having a pitch length of 42.3 inches is selected.

Belt speed is given by:

$$V = \frac{\pi d n_1}{12} = \frac{\pi x 3.4 x 1150}{12} = 1025 \text{ fpm.} \qquad (2.13)$$

From Table 15.9 of Ref. (3), the rated H.P. per belt is 0.81. This must be corrected for the contact angle and the belt length. The contact angle for the small sheave is 140.2°. From Fig. 15.5 of Ref. (3), the correction factor is 0.89. The belt length correction factor is 0.85 from the Table 15.10 of Ref. (3). Therefore, the H.P. per belt is:

$$\text{H.P. per belt} = 0.81 \times 0.89 \times 0.85 = 0.6125$$

$$\text{Number of belts required} = \frac{\text{Total H.P.}}{\text{H.P. per belt}} = 2.45$$

Making allowances for incertainties and variations in the load, three A42 belts would be used. An approximate center distance can be calculated from Eq. (2.12). The center distance should be adjusted according to required tension in the belt, the method of tensioning being given in a typical manufacturer's catalogue.

A slide motor base is selected to facilitate the installation of v-belts and adjustment of the center distance.

C. Flywheel Design

The flywheel is required for maintaining a nearly constant drive shaft speed. The larger the flywheel inertia, the smaller will be the variation in the drive shaft velocity, hence, the smaller the variations from sinusoidal velocity in the driven shaft. The mass moment

of inertia of the flywheel was chosen to be about 30 lb-in-sec^2, based on a guideline found adequate by Ashar[2]. He found that a flywheel inertia of one or two orders of magnitude greater than the driven side inertia would keep the coefficient of fluctuation of the drive shaft speed at about 0.006.

A solid disc flywheel design was chosen which incorporates the ability to incrementally change its mass moment of inertia by addition or subtraction of segments, ΔI_f being approximately 12 lb-in-sec^2.

Figure 2.3 shows two views of the solid disc flywheel. Figure 2.4 shows two views of the segments which are used to change the flywheel's mass moment of inertia. Two or four such segments can be used on each side of the disc flywheel. The flywheel is fastened by bolts to a flange which is welded to the drive shaft. Figure 2.5 shows two views of this flange.

It is known that in case of a rotating body, the slightest unbalance may produce a very large disturbing force. Due to errors in machining and non-homogeneity of the material, it would be difficult to manufacture a perfectly balanced flywheel. Hence, balancing would be necessary when using the flywheel without segments as well as with segments.

1. Flywheel Inertia

The mass moment of inertia of the flywheel, neglecting the effect of bolt holes, about its axis is given by:

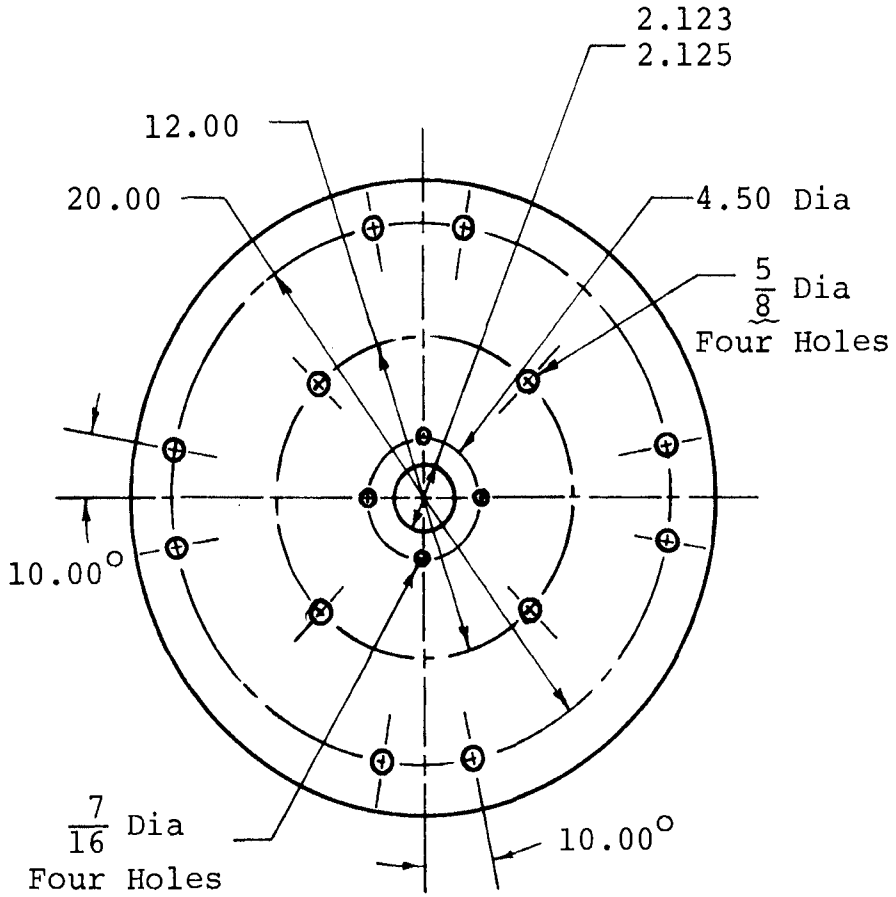

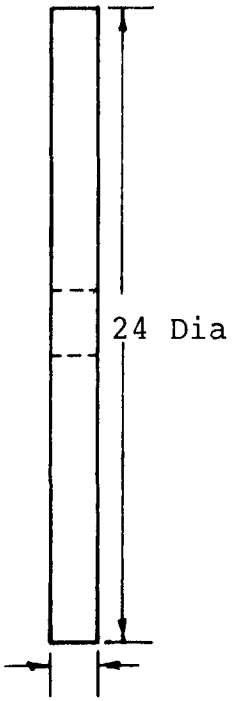

Material-Steel

Fig. 2.3 Flywheel

Scale- 1:8

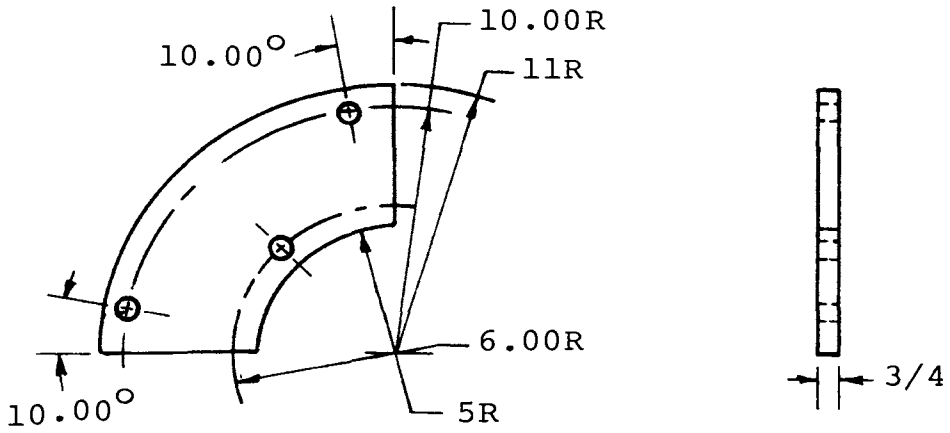

Material-Steel Fig. 2.4. Flywheel Segment Scale- 1:8

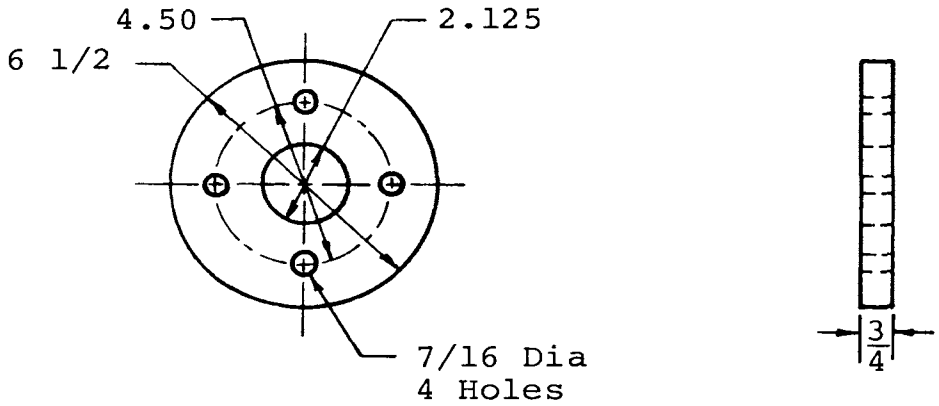

Material-Steel Fig. 2.5. Flange Scale- 1:5

$$I_f = W/g \times R^2/2 \qquad (2.14)$$

where

I_f = Mass moment of inertia of the disc flywheel, lb-in-sec^2

W = Weight of the solid disc, lbs.

R = Radius of the disc, in.

g = Gravitational constant, in/sec^2

Substituting W = 254 lbs., R = 12 in., and g = 386 in/sec^2 into Eq. (2.14) gives:

$$I_f = \frac{254 \times 12^2}{386 \times 2} = 47.4 \text{ lb-in-sec}^2$$

The combined mass moment of inertia of the solid disc flywheel and the segments is given by:

$$I_{fs} = I_f + I_s \qquad (2.15)$$

where:

I_{fs} = Combined mass moment of inertia of the disc flywheel and segments,

I_s = Mass moment of inertia due to segments, lb-in-sec^2

The mass moment of inertia due to each segment may be approximated as one fourth the mass moment of inertia of an annular ring with R_s and r_s as the outer and inner radii, respectively. It is given by:

$$I_s = 1/4 \left(\frac{W_r}{g} \times \frac{(R_s^2 + r_s^2)}{2} \right) \qquad (2.16)$$

where

W_r = Weight of the annular ring, lbs.

R_s = Outer radius of the annular ring, in.

r_s = Inner radius of the annular ring, in.

Substituting W_r = 63.25 lbs., R_s = 11 in., r_s = 5 in. and g = 386 in/sec^2 into Eq. (2.16), gives:

$$I_s = 1/4 \left[\frac{63.25}{386} \left(\frac{11^2 + 5^2}{2} \right) \right] = 3 \text{ lb-in-sec}^2$$

The different flywheel inertias which can be obtained with this type of flywheel are given in Table I.

2. Bolt Stresses

The stresses in the flange bolts and segment bolts are calculated to make sure that they are within the safe limit.

(a) Flange Bolts

Figure 2.6 shows the flywheel-flange joint. The stresses in the flange bolt are due to torque only. For the motor selected, the torque decreases as the speed increases. Assuming that the full torque is exerted, the maximum torque at 370 RPM is calculated to be 255 lb-in. The shear load in the bolt due to this torque is:

TABLE I

VALUES OF FLYWHEEL INERTIAS

Nomenclature	No. of Segments	Mass Moment of Inertia ($lb\text{-}in\text{-}sec^2$)
I_f*	Zero (Disc flywheel)	47.4
I_{f1}	Four (Two Segments on each side of the disc flywheel)	59.4
I_{f2}	Eight (Four segments on each side of the disc flywheel)	71.4

* $I_f > I_f$ minimum suggested by Ashar

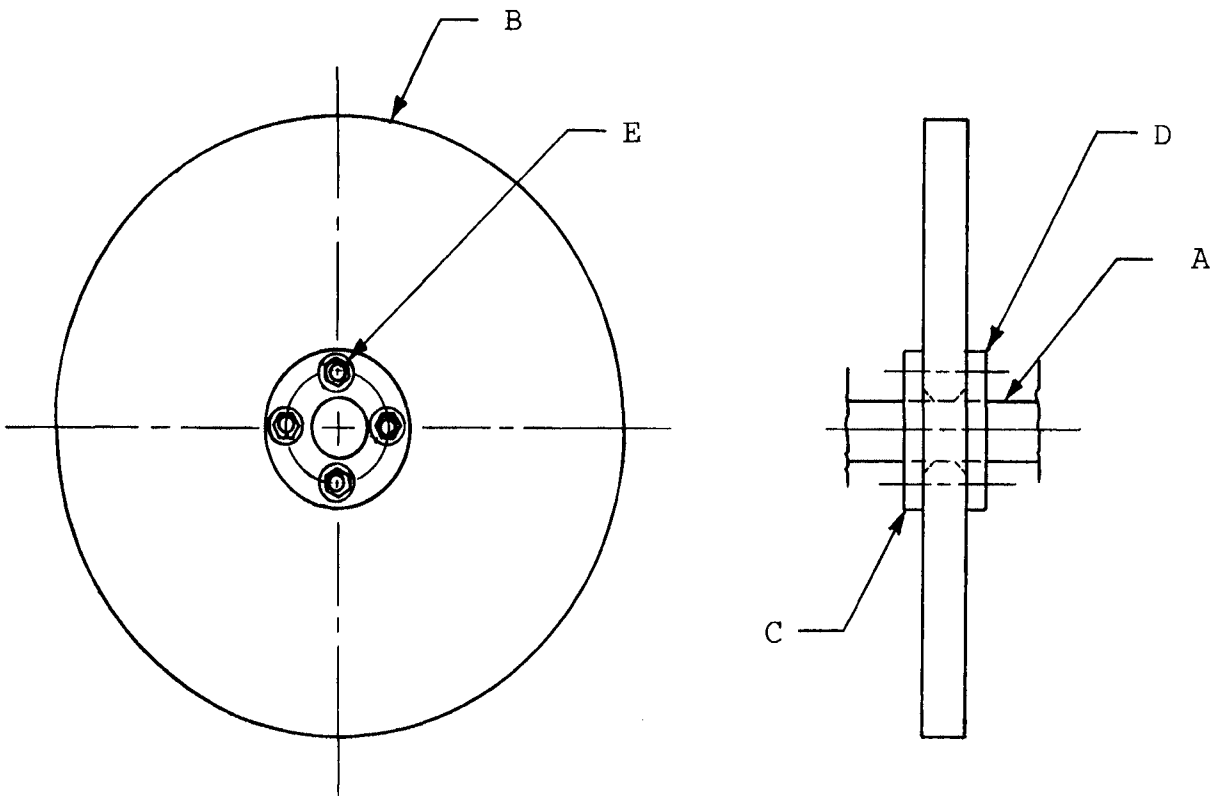

A Drive Shaft

B Flywheel

C Flange

D Flange (welded to the shaft)

E Flange Bolts ($\frac{7}{16}$ -14UNC-2A/2B) at 2.25R

Fig. 2.6 Flywheel - Flange Joint

$$F_f = \frac{255}{(2.25)(4)} = 28.3 \text{ lbs.}$$

Therefore, the maximum shearing stress is given by:

$$f_{sf} = \frac{4}{3}\left(\frac{F_f}{2A_f}\right) \tag{2.17}$$

where:

f_{sf} = Maximum shearing stress, psi

A_f = Bolt minor diameter area, in^2

Substituting $F_f = 28.3$ lbs., $A_f = 0.0933$ in^2 into Eq. (2.17), gives

$$f_{sf} = \frac{4}{3}\left[\frac{28.3}{2(0.0933)}\right] = 204 \text{ psi}$$

Assuming that one bolt carries the entire shear load, the factor of safety is given by: (3)

$$n = \frac{\text{yield strength in shear}}{\text{shear stress}} = \frac{(.55)(\text{proof load})}{\text{shear stress}} \tag{2.18}$$

$$= \frac{(0.55)(55{,}000)}{(204)} = 148$$

It may be argued that the initial tensile stress (due to preload) in the bolt should be combined with the shear stress and then the factor of safety be found by using the principal stresses. But it must be remembered that the shear load cannot actually come on the bolt until the frictional force between the mating surfaces (due to preload in the bolt) is overcome. Consequently, the two

stresses will not exist simultaneously. The recommended preload for this particular joint is calculated to be about 500 pounds, which will create sufficient friction between the assembled members so that no slippage occurs. Thus, a very strong, reliable joint can be obtained if care is taken in the assembly of the joint. Thick, hardened steel washers should be used under the nut and bolt head to distribute compression uniformly. The mating surfaces should be parallel, flat, dry, and unlubricated.

(b) Segment bolts

The stresses in the bolts attaching the flywheel segment to the disc flywheel result from the superposition of centrifugal force, inertia force from flywheel speed variation, and bolt preload. The stresses due to inertia force will be small, as only a slight variation is allowable in the flywheel speed. For this reason, stresses due to centrifugal force only are considered, assuming that no friction force between the flywheel and flywheel segment is present, i.e., bolt preload is zero. The maximum RPM of the flywheel, in this specific design, is limited to about 1000 RPM, but for safety the stresses are checked for possible operation at 2000 RPM. The centrifugal force on each segment at this speed is given by:

$$C_f = W_s/g \times a \qquad (2.19)$$

where:

C_f = Centrifugal force on each segment, lbs.

W_s = Weight of the segment, lbs.

a = Normal acceleration, in/sec^2

$$= 0.6 \times \frac{(R_s^3 - r_s^3)}{(R_s^2 - r_s^2)} \omega_2^2$$

$$= .6 \times \frac{(11^3 - 5^3)}{(11^2 - 5^2)} \times \left(\frac{2x\pi x2000}{60}\right)^2 = 33.2x10^4 \text{ in/sec}^2$$

$$C_f = \frac{15.8}{386} \times 33.2x10^4 = 13600 \text{ lbs.}$$

The centrifugal force on each bolt is 4533 lbs. Assuming the bolt in direct shear, the maximum shearing stress is:

$$f_{ss} = \frac{4}{3} \times C_f/A_r = \frac{4}{3} \times \frac{4533}{0.202} \cong 30{,}000 \text{ psi} \qquad (2.20)$$

where:

f_{ss} = Maximum shearing stress, psi

A_r = Bolt minor diameter area, in^2

Assuming that one bolt carries the entire shear load, the factor of safety is:

$$n = \frac{\text{yield strength in shear}}{\text{shear stress}} = \frac{66{,}000}{30{,}000} \cong 2 \qquad (2.21)$$

The preload in the bolt, which should be about 10,800 psi, would prevent slippage between the assembled parts. Thus, the shear load would not occur on the bolt (see Fig. 2.4) until the initial tension due to preload is relieved.

3. Flywheel Stresses

The tangential and radial stresses[4] for a rotating disc with a hole at the center are given by:

$$f_t = C\rho N^2[(3+\lambda)\{R^2+r^2+(R^2r^2/r_1^2)\}-(1+3\lambda)r_1^2] \qquad (2.22)$$

$$f_r = C\rho N^2[(3+\lambda)\{R^2+r^2-(R^2r^2/r_1^2)\}] \qquad (2.23)$$

where:

f_t = Tangential stress, psi

f_r = Radial stress, psi

C = A constant = 0.00000355

N = Speed, RPM

ρ = Density of the material of the flywheel, lb/in^3

λ = Poisson's ratio

R = Outer radius of the disc, in.

r_1 = Inner radius of the disc, in.

Substituting N = 2000 RPM, ρ = 0.28 lb/in^3, R = 12 in., r = 1.25 in., r_1 = 1.25 in., λ = 0.3 for steel, the maximum stresses which occur at the inner radius are:

$$f_t = \frac{355}{10^8} \times 0.28\times2000^2[(3+.3)\{12^2+1.25^2+12^2\}-(1+0.9)1.25^2]$$

$$= 3790 \text{ psi}$$

$$f_r = \frac{355}{10^8} \times 0.28\times2000^2[(3+.3)\{12^2+1.25^2-12^2\}] = 20.45 \text{ psi}$$

These stresses are considerably lower than the yield stresses of the material.

D. Drive Shaft

A 2 inch diameter steel shaft was tentatively selected as a basis for the analysis. The fundamental torsional frequency, as per the design criterion chosen, should be about five times the maximum forcing frequency applied to the specimen. The maximum RPM of the flywheel is taken to be approximately 1000 RPM which defines the output forcing frequency to be 33.3 cps. Therefore, the natural frequency of the shaft should be greater than 150 cps.

The detailed dimensions of the shaft were determined so as to be compatible with standard bearings, v-belt sheaves and the Hooke's joint. Figure 2.7 gives the complete dimensions for this shaft.

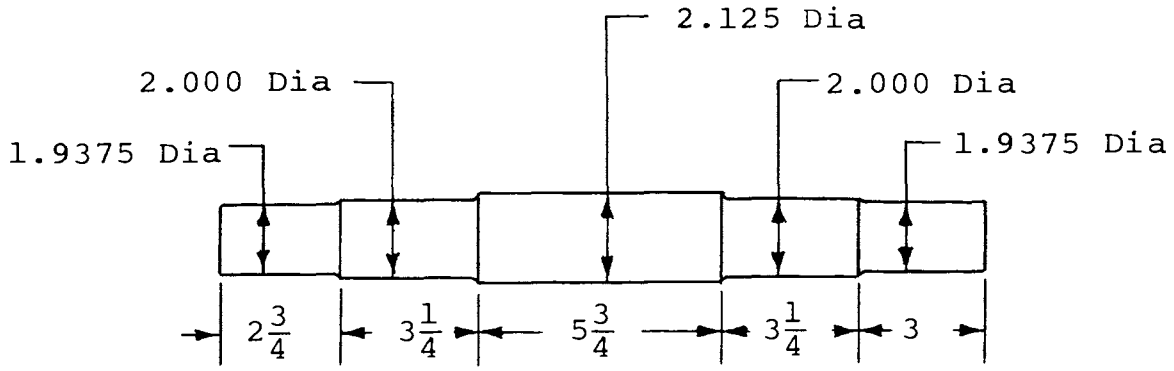

Material-Steel Fig. 2.7 Drive Shaft Scale- 1:5

1. Torsional Vibration of the Shaft

The actual system can be treated as a spring mass system as shown in Fig. 2.8. The frequency equation for such a system is given by:[5]

$$\omega_t^2[I_1 I_{f2} I_d \omega_t^4 - \{(I_1 I_{f2} + I_1 I_d)k_{fd} + (I_{f2} I_d + I_1 I_d)k_{1f}\}\omega_t^2 + k_{1f} k_{fd}(I_1 + I_{f2} + I_d)] = 0 \quad (2.24)$$

where:

ω_t = Natural frequency of torsional vibration, rad/sec

I_1 = Mass moment of inertia of the large sheave, lb-in-sec^2

I_{f2} = Mass moment of inertia of the flywheel with segments, lb-in-sec^2

I_d = Mass moment of inertia of the driven side, lb-in-sec^2

k_{1f} = Torsional stiffness of the shaft between the flywheel and the large sheave, lb-in/rad

k_{fd} = Torsional stiffness of the shaft between the flywheel and the Hooke's joint, lb-in/rad

Equation (2.24) is a cubic equation in ω_t^2 of which one of the roots is zero. This root corresponds to the possibility of having the shaft rotate as a rigid body without any torsion. The other two roots can be found from the quadratic equation:

$$I_1 I_{f2} I_d \omega_t^4 - \{(I_1 I_{f2} + I_1 I_d)k_{fd} + (I_{f2} I_d + I_1 I_d)k_{1f}\}\omega_t^2 + k_{1f} k_{fd}(I_1 + I_{f2} + I_d) = 0 \quad (2.25)$$

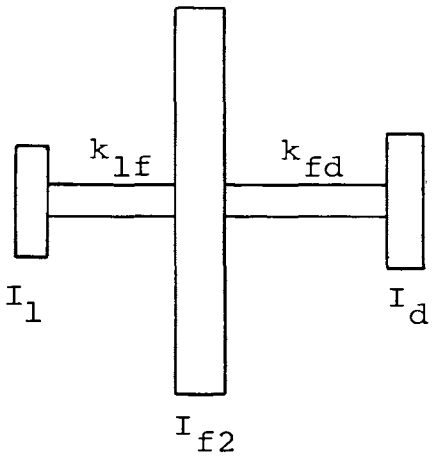

I_l - Mass moment of inertia of the large sheave

k_{lf} - Torsional stiffness of the shaft between the large sheave and the flywheel

I_{f2} - Mass moment of inertia of the flywheel with segments

k_{fd} - Torsional stiffness of the shaft between the flywheel and the driven side

I_d - Mass moment of inertia of the driven side

Fig. 2.8 Equivalent System for Torsional Vibrations of the Drive Shaft

The mass moment of inertia of the large sheave, I_l, is calculated to be 0.4 lb-in-sec^2 according to the procedure given in a typical manufacturer's catalogue. The torsional stiffness of the shaft between the large sheave and the flywheel, k_{lf}, and the torsional stiffness of the shaft between the flywheel and the Hooke's joint, k_{fd}, are calculated, assuming a uniform equivalent shaft, to be 2.5×10^6 lb-in/rad and 3.25×10^6 lb-in/rad, respectively. An equivalent shaft has a uniform diameter and has the same spring constant as the actual stepped shaft. The mass moment of inertia of the driven side, I_d, would consist of the mass moment of inertia of the driven shaft and a specimen. For a particular specimen rigidly connected to the driven shaft through a rigid coupling, I_d, is calculated to be 0.7 lb-in-sec^2. Taking into account that specimens of higher mass moment of inertia may be tested, I_d is assumed to be 2.5 lb-in-sec^2. Also, $I_{f2} = 71.4$ lb-in-sec^2. Substituting these values into Eq. (2.25) and solving, gives $f_{t1} = 237$ cps and $f_{t2} = 382$ cps. The lowest frequency is 237 cps and is acceptable within the design criteria.

2. Lateral Vibration of the Shaft

The vibration system considered for the drive shaft assembly is shown in Fig. 2.9. In this calculation the weight of the driver sheave, being only 6% of the flywheel weight, was neglected and a uniform cross section shaft

was assumed.

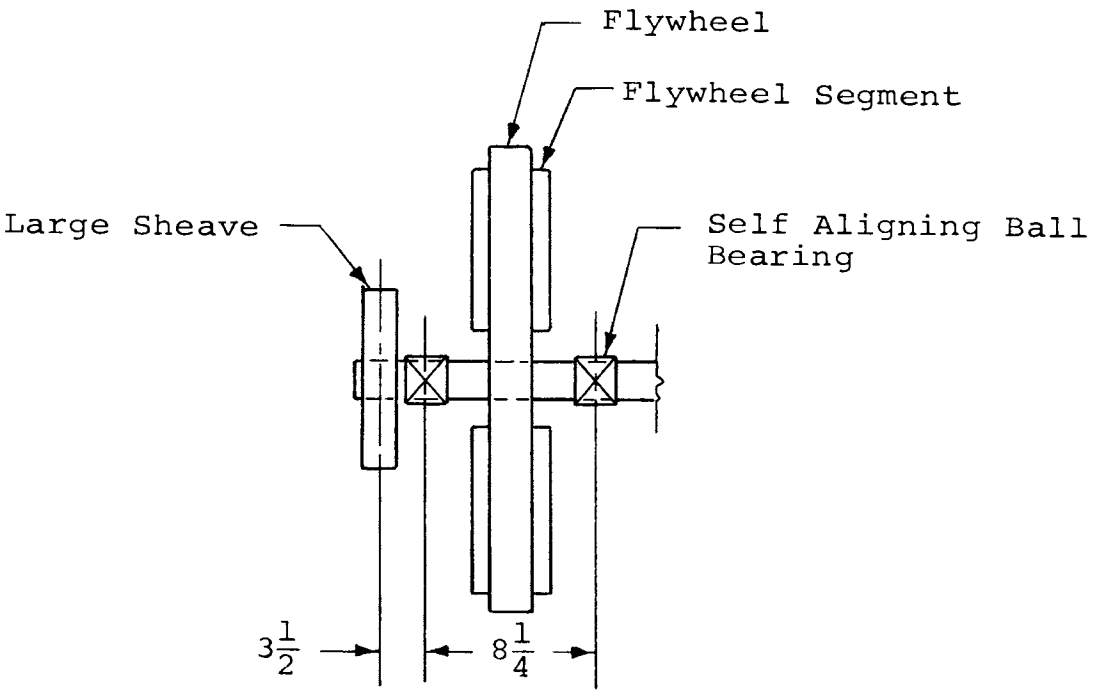

Fig. 2.9 Flywheel-Bearings Arrangement

The natural frequency of lateral vibration of the shaft can be calculated with fair accuracy from its static deflection curve and is given by:

$$f_L = \frac{1}{2\pi} \sqrt{\frac{g k_l}{W_f}} \qquad (2.26)$$

where:

f_L = Natural frequency of lateral vibration of the shaft, cps

W_f = Total weight of the flywheel, lbs.

k_l = Lateral stiffness of the shaft, lb/in.

Substituting g = 386 in/sec^2, k_1 = 2.98 x 10^6 lb/in and W_f = 380 lbs into Eq. (2.26), gives:

$$f_L = \frac{1}{2\pi} \sqrt{\frac{386 \times 2.98 \times 10^6}{380}} = 277 \text{ cps}$$

This frequency is acceptable as per the design criterion.

3. Belt Flexibility

The power is transmitted through three "A" section v-belts. The action of the belts, due to flexibility, is like a torsional spring. Considering this action, the natural frequency of torsional vibration of the system shown in Fig. 2.10 is calculated. This frequency, as per the design criterion, should be above 150 cps which insures that the belts are stiff enough for the specific purpose.

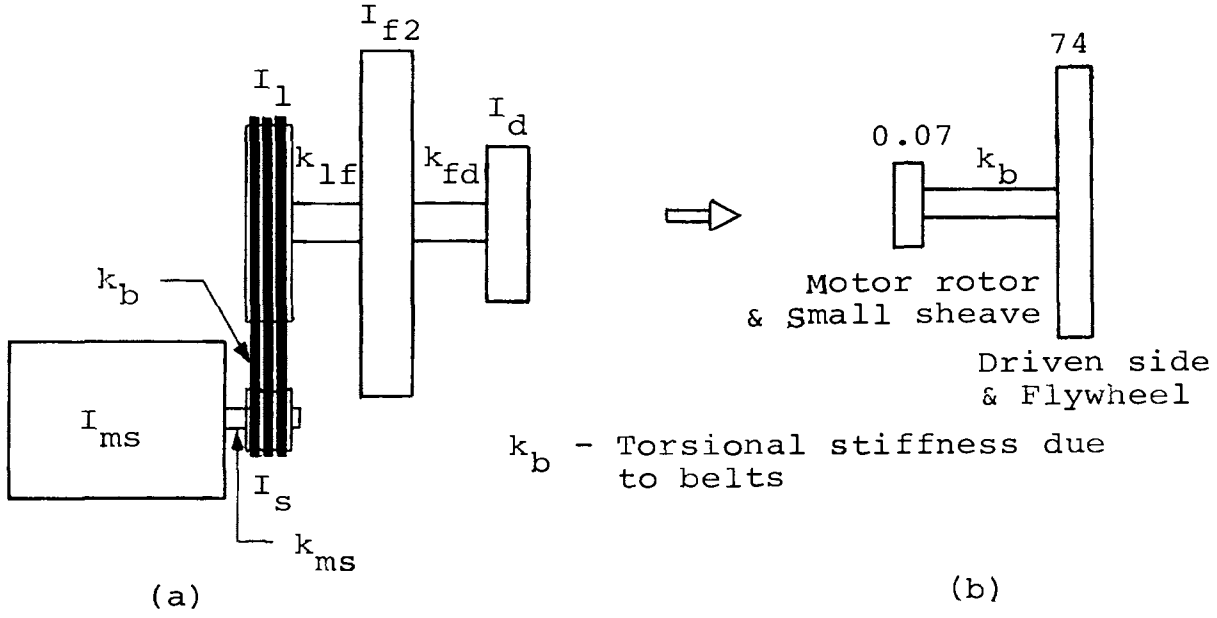

Fig. 2.10 System to Check Belt Vibrations

The values and descriptions of the parameters in Fig. 2.10 are given in Table II. As k_{ms}, k_{lf} and k_{fd} are considerably higher than k_b [6], the actual system can be approximated by that shown in Fig. 2.10(b). The approximate fundamental frequency is calculated to be 147 cps. The belt flexibility can be increased by increasing the number of belts or by using larger cross section belts. For this specific machine the transmission system should be acceptable.

E. Selection of Bearings

Self aligning ball bearings were selected to support the drive shaft. This type of bearing incorporates minimum clearance and actual friction for all practical purposes is negligible. The bearing load consists of the load from the v-belt drive, load due to the flywheel weight and load due to bending moment on the drive shaft when the shafts of the Hooke's joint are at an angle other than zero.

1. Load from V-Belt Drive

This load as calculated according to the method given in a typical manufacturer's catalogue is 72 lbs. The bearing loads are computed using the indicated distances between bearings and loads as shown in Fig. 2.11.

$$\text{Load on Bearing I} = \frac{72 \times 3.5}{8.25} = 30.6 \text{ lbs.}$$

$$\text{Load on Bearing II} = \frac{72 \times 11.75}{8.25} = 102.5 \text{ lbs.}$$

TABLE II

VALUES OF PARAMETERS IN FIGURE 2.10

Parameter	Description	Value
I_{ms}	Mass moment of inertia of the rotor	0.04 lb-in-sec^2
I_s	Mass moment of inertia of the small sheave	0.03 lb-in-sec^2
I_l	Mass moment of inertia of the large sheave	0.4 lb-in-sec^2
I_{f2}	Mass moment of inertia of the flywheel with segments	71.4 lb-in-sec^2
k_{ms}	Torsional stiffness of the motor shaft	0.3x10^{6}lb-in/rad
k_b	Torsional stiffness due to 3 belts	0.06x10^{6}lb-in/rad
k_{lf}	Torsional stiffness of the shaft between the large sheave and the flywheel	2.5x10^{6}lb-in/rad
k_{fd}	Torsional stiffness of the shaft between the flywheel and Hooke's joint	3.25x10^{6}lb-in/rad
I_d	Mass moment of inertia of the driven side	2.5 lb-in-sec^2

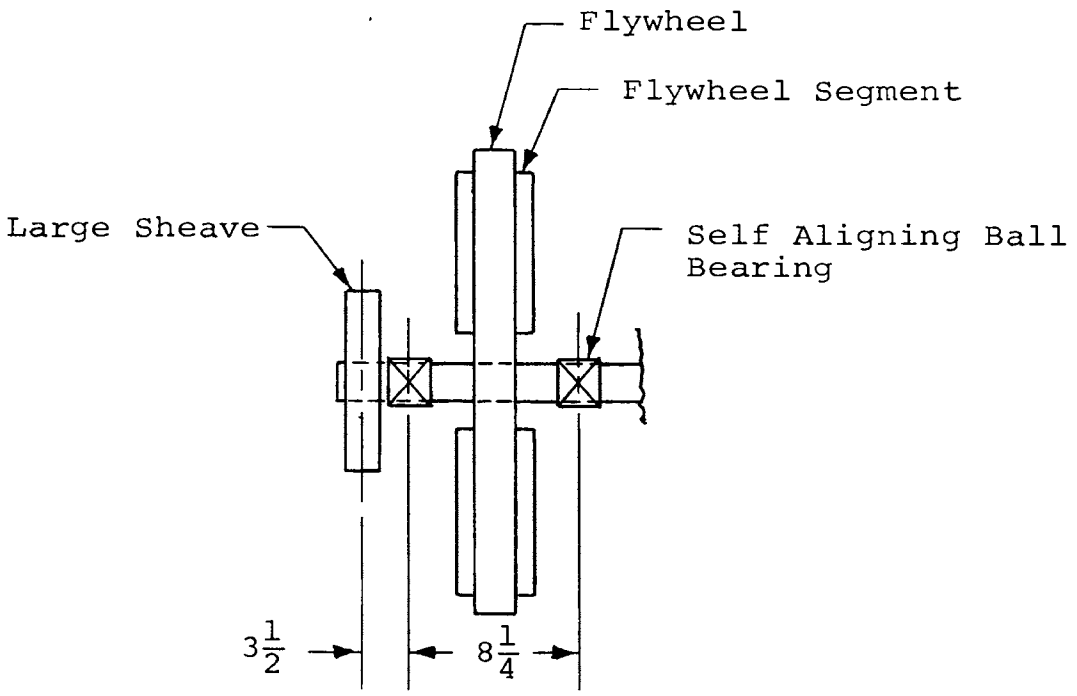

Fig. 2.11 Flywheel-Bearings Arrangement

2. Load Due to the Flywheel Weight

The load on each bearing due to the flywheel weight is 190 lbs.

3. Load Due to Bending Moment

This load is induced due to a bending moment in the drive shaft when the included angle β of the Hooke's joint is other than zero. The load is maximum when the bending moment is maximum[7]. Figure 2.12(a) shows the paths of yoke arms of a Hooke's joint. Figure 2.12(b) represents the torque transmitted from one shaft to the other through the cross arm.

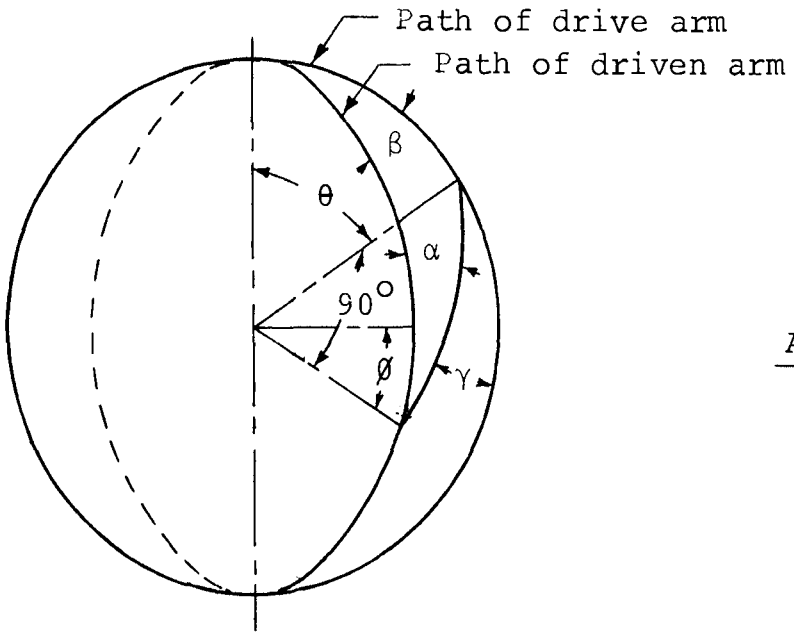

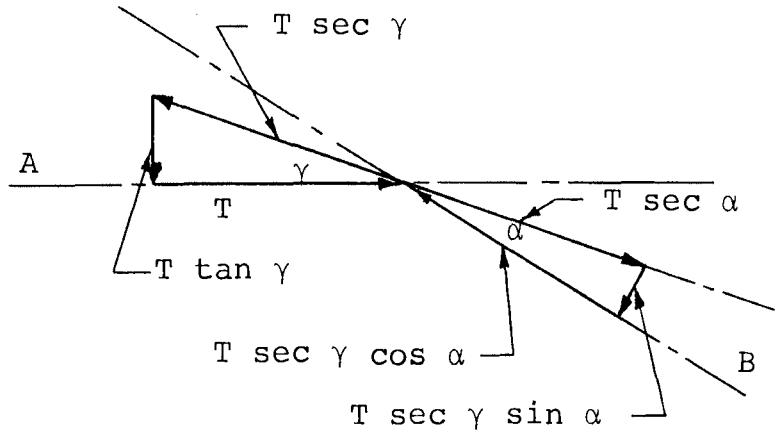

β = Spherical angle between shafts

θ = Angle of rotation of drive shaft

Ø = Angle of rotation of driven shaft

α = Angle of rotation of bearing on driven yoke from θ = 0°

γ = Angle of rotation of bearing on driving yoke from θ = 0°

A - Drive Shaft

B - Driven Shaft

T - Torque in the drive shaft

Fig. 2.12a Paths of Yoke Arms for Drive and Driven Shafts of a Hooke's Joint

Fig. 2.12b Torques Transmitted from a Drive Shaft to Driven Shaft of a Hooke's Joint

$$\text{Maximum bending moment} = T \tan \gamma = T \tan \beta \qquad (2.27)$$

where:

T = Torque in the drive shaft, lb-in

β = Hooke's joint angle, degree

Substituting T = 256 lb-in and $\beta = 20^{o}$ into Eq. (2.27) gives:

Maximum bending moment = 256 x tan 20 = 93 lb-in.

Load on each bearing due to the bending moment is:

$$\frac{\text{Bending moment}}{\text{Distance between bearings}} = \frac{93}{8.25} = 11.25 \text{ lbs.}$$

The maximum bearing load, on bearing II, is 303.75 lbs. Taking into account vibration loads etc., the maximum load is assumed as 500 lbs. From the manufacturer's catalogue the Minimum Hours of Life is found to be about 30,000 hours for the bearing selected. At high speeds, the load is reduced and Life increased. Thus, the selected bearings would give satisfactory performance for a long period.

F. Bearing Supports

Two types of support structures for the bearings were examined. Both of these designs were analyzed to determine the natural frequencies in rocking and torsion type of dynamic deflection modes. The system shown in Fig. 2.13 was considered for vibration analysis. For

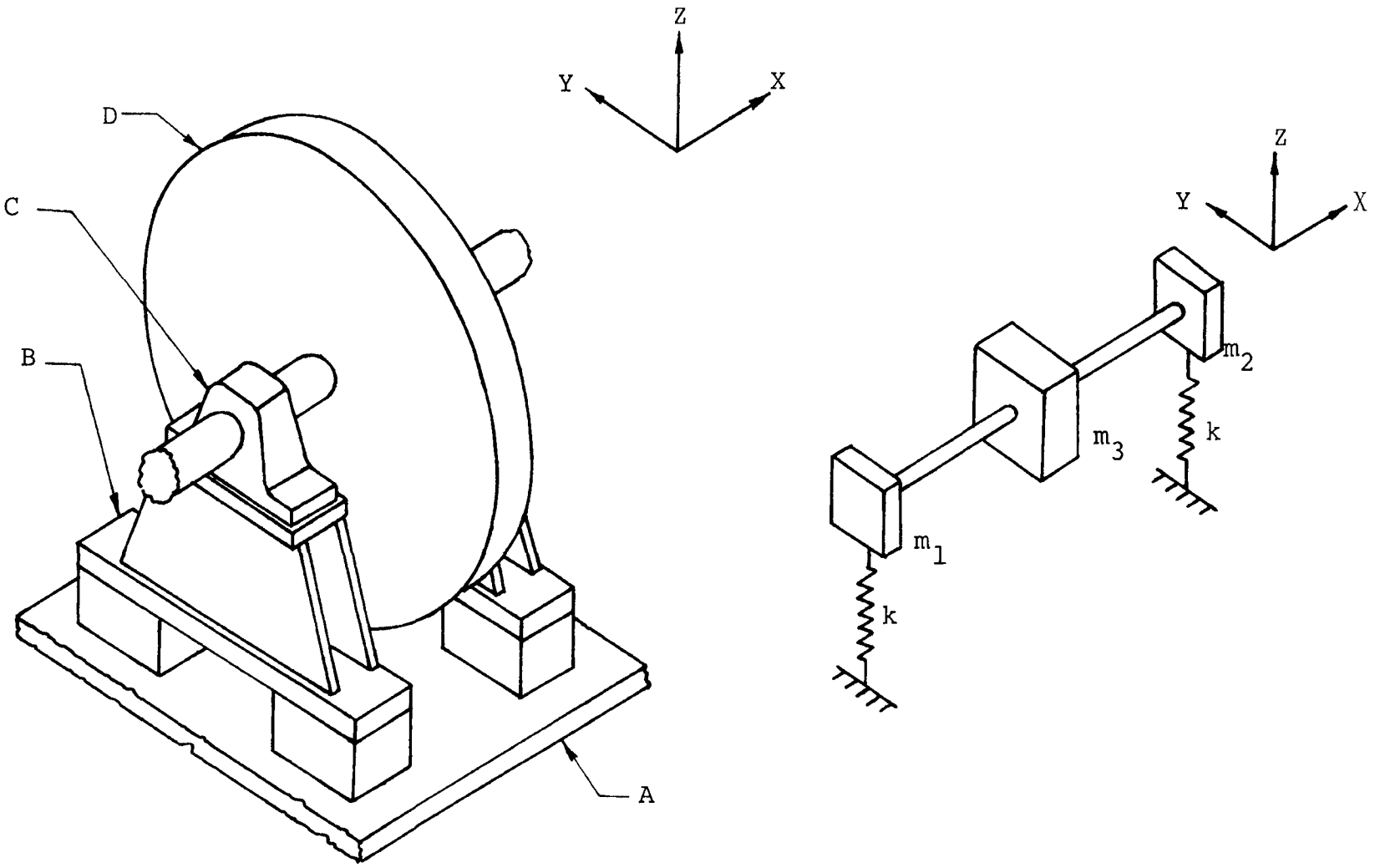

Fig. 2.13. Drive Side Vibration System

In Fig. 2.13,

A	Drive Plate
B	Drive Shaft Bearing Support
C	Drive Shaft Bearing
D	Flywheel
k	Spring Stiffness of the Bearing Support
m_1, m_2	1/3 weight of the bearing support + 1/3 weight of the drive shaft + weight of the upper plate of the bearing support + weight of the bearing.
m_3	Weight of the flywheel with segments

each mode the actual system was converted into a discrete spring-mass system model and frequencies were calculated for these simplified models. Dunkereley's equation[8] was used to couple these modes and find an approximation of the fundamental natural frequency of the system. Figure 2.14 shows three views of the bearing support structure which was considered.

1. Longitudinal Rocking Mode

The discrete spring-mass model and the respective deflection mode is shown in Fig. 2.15. The natural frequency of this simplified model of the system is given by:

$$f_1 = \frac{1}{2\pi} \sqrt{\frac{2k_1 \times g}{m_1+m_2+m_3}} \qquad (2.28)$$

where:

f_1 = Natural frequency of vibration of the system in longitudinal rocking mode, cps

k_1 = Spring stiffness of the bearing support in the longitudinal direction, lb/in

$m_1 = m_2$ = 1/3 weight of the bearing support + 1/3 weight of the shaft + weight of the upper plate of the bearing support + weight of the bearing, lbs.

m_3 = Weight of the flywheel with segments, lbs.

The spring stiffness of the bearing support is calculated by treating the support as a cantilever beam where the major deflections in this rocking mode are in

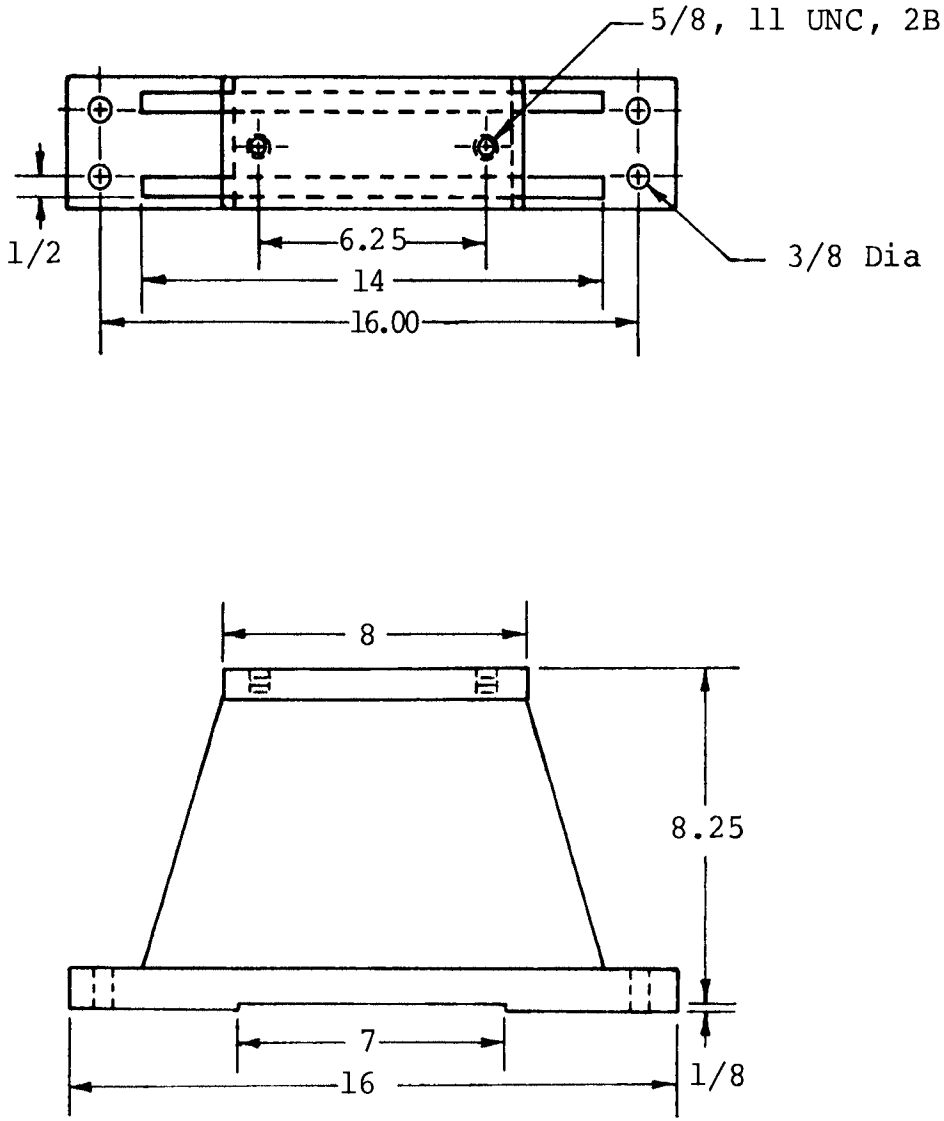

Fig. 2.14. Drive Shaft Bearing Support (Type 1)

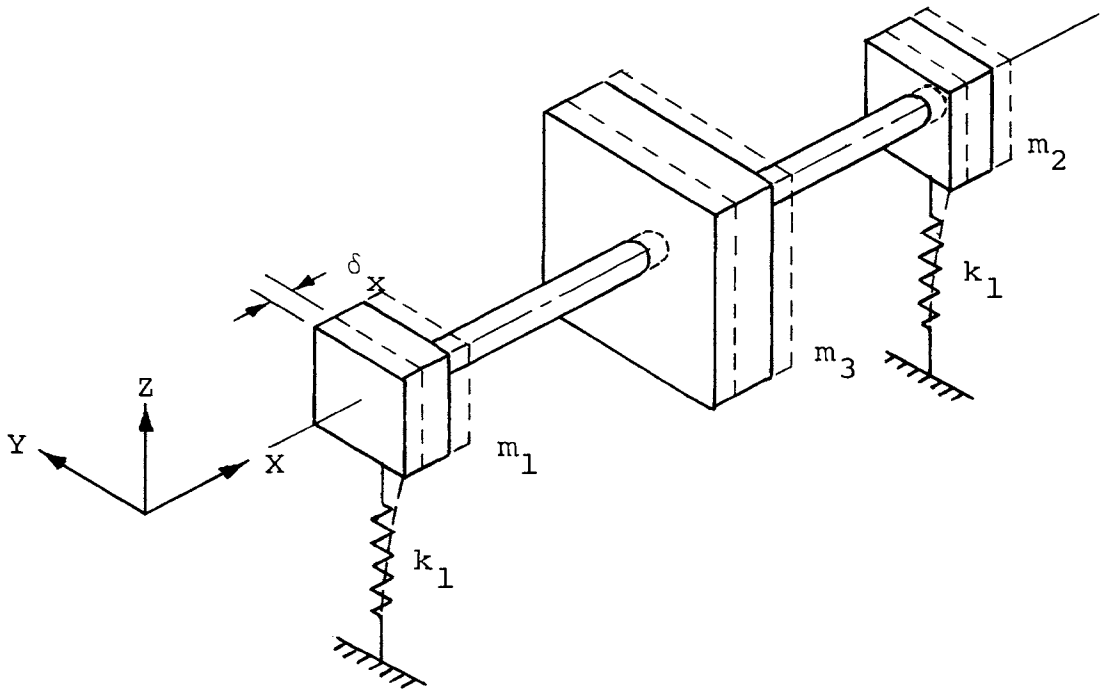

k_1 - Longitudinal spring stiffness of the bearing support

m_1, m_2 $\frac{1}{3}$ weight of the bearing support + $\frac{1}{3}$ weight of the shaft + weight of the upper plate of the bearing support + weight of the bearing

m_3 - Weight of the flywheel, with segments

δ_x - Deflection in x-direction

Fig. 2.15 Longitudinal Rocking Mode

the direction of the flywheel shaft. Also, average cross sectional properties of the support are used to simplify the analysis. The simplification is justified as the design frequency is high enough and exact analysis is not needed. Substituting $k_1 = 3.26 \times 10^6$ lb/in, $m_1 = m_2 = 23$ lbs., and $m_3 = 385$ lbs. into Eq. (2.28), gives:

$$f_1 = \frac{1}{2\pi} \sqrt{\frac{2 \times 3.26 \times 10^6 \times 386}{431}} = 385 \text{ cps}$$

2. Transverse Rocking Mode

For this mode the major deflections are in the Y-direction as shown in Fig. 2.16. The natural frequency of this simplified model is given by:

$$f_2 = \frac{1}{2\pi} \sqrt{\frac{2k_2 \times g}{m_1+m_2+m_3}} \qquad (2.29)$$

where:

f_2 = Natural frequency of vibration of the system in transverse rocking mode, cps

k_2 = Spring stiffness of the bearing support in Y-direction, lb/in.

Substituting $k_2 = 27.35 \times 10^6$ lb/in. as calculated by treating the support as cantilever beam and using average cross sectional properties, $m_1 = m_2 = 23$ lbs., and $m_3 = 385$ lbs. into Eq. (2.29), gives:

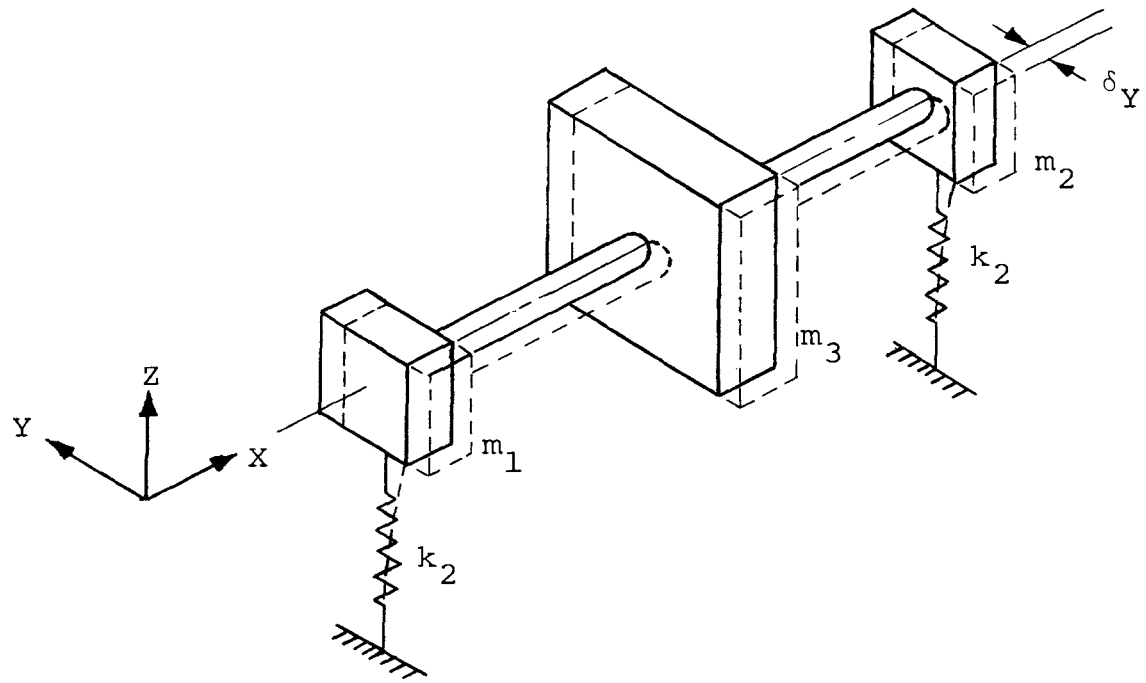

k_2 - Transverse spring stiffness of the bearing support

m_1, m_2 - 1/3 weight of the bearing support + 1/3 weight of the shaft + weight of the upper plate of the bearing support + weight of the bearing

m_3 - Weight of the flywheel with segments

δ_Y - Deflection in Y-direction

Fig. 2.16 Transverse Rocking Mode

$$f_2 = \frac{1}{2\pi}\sqrt{\frac{2 \times 27.35 \times 10^6 \times 386}{431}} = 1114 \text{ cps}$$

3. Torsional Mode

In this mode the system may rotate in the XY-plane as shown in Fig. 2.17. The natural frequency of this simplified model of the system is given by:

$$f_3 = \frac{1}{2\pi}\sqrt{\frac{2k_3\, l^2}{I + \frac{m_1'}{g} l^2 + \frac{m_2'}{g} l^2}} \qquad (2.30)$$

where:

f_3 = Natural frequency of vibration of the system in torsional mode, cps

$k_3 = k_2$ = Spring stiffness of the bearing support in Y-direction, lb/in

$m_1' = m_2'$ = 1/3 weight of the bearing support + weight of the upper plate of the support + weight of the bearing, lbs.

I = Mass moment of inertia of the flywheel about its diameter + mass moment of inertia of the shaft about the axis at its mid length, lb-in-sec^2

l = 1/2 the distance between the bearings, in.

Substituting $k_3 = 27.35 \times 10^6$ lb/in., $m_1' = m_2' = 18$ lbs., I = 36.44 lb-in-sec^2 and l = 4.12 in. into Eq. (2.30), gives:

$$f_3 = \frac{1}{2\pi}\sqrt{\frac{2 \times 27.35 \times 10^6 \times (4.12)^2}{36.44}} = 797.5 \text{ cps}$$

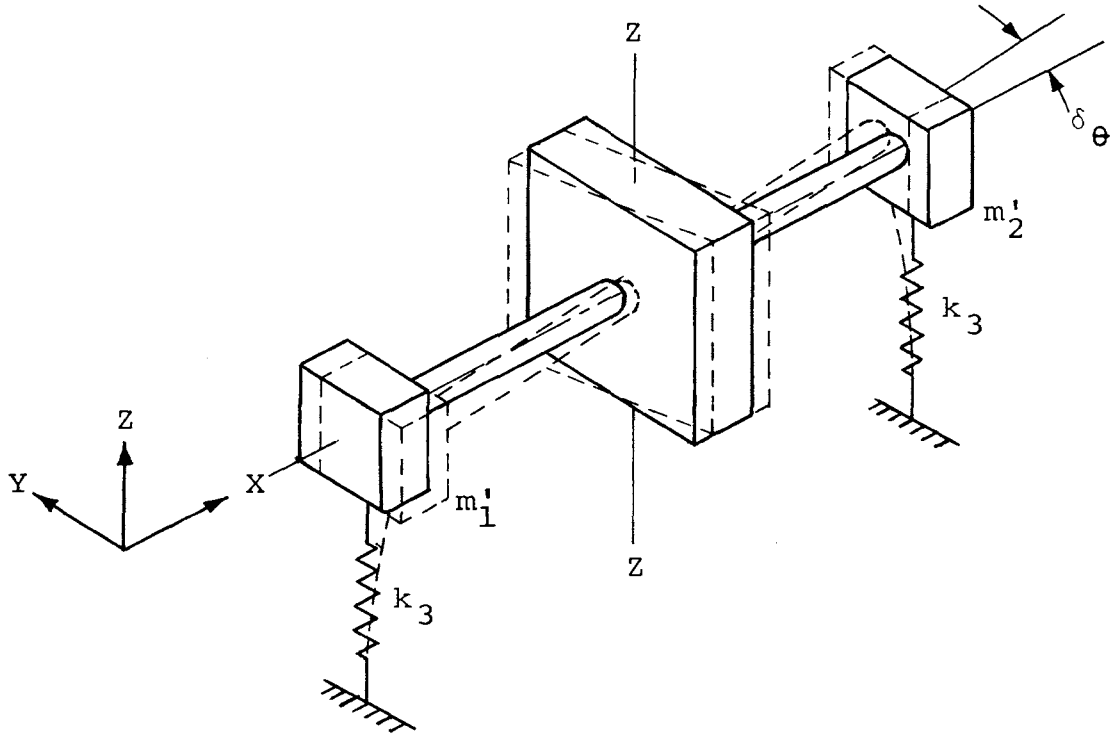

k_3 - Transverse spring stiffness of the bearing support

m_1', m_2' - 1/3 weight of the bearing support + weight of the upper plate of the support + weight of the bearing

δ_θ - Rotation of the system in X-Y plane about Z-axis

Fig. 2.17 Torsional Mode

4. Fundamental Natural Frequency

An approximation for the fundamental natural frequency can be obtained by using Dunkereley's equation[8]. The approximate equation for the fundamental frequency can be written as:

$$1/f^2 = 1/f_L^2 + 1/f_1^2 + 1/f_2^2 + 1/f_3^2 \qquad (2.31)$$

where f_L is the natural frequency of lateral vibration of the drive shaft and f_1, f_2, f_3 are the natural frequencies of the system corresponding to each uncoupled mode as calculated in the three previous sub-sections. Substituting f_L = 277 cps, f_1 = 385 cps, f_2 = 1114 cps and f_3 = 797.5 cps into Eq. (2.31), gives:

$$1/f^2 = \frac{1}{(277)^2} + \frac{1}{(385)^2} + \frac{1}{(1114)^2} + \frac{1}{(797.5)^2}$$

or

$$f = 213 \text{ cps}$$

The natural frequencies of vibration of the system when using the second type of support as shown in Fig. 2.18 are:

f_1 = 237 cps (Longitudinal Rocking Mode)

f_2 = 1410 cps (Transverse Rocking Mode)

f_3 = 1020 cps (Torsional Mode)

and the combined fundamental frequency is f = 176 cps. The comparison of results shows that the type 1 support is stiffer than the type 2 and, hence, should be selected.

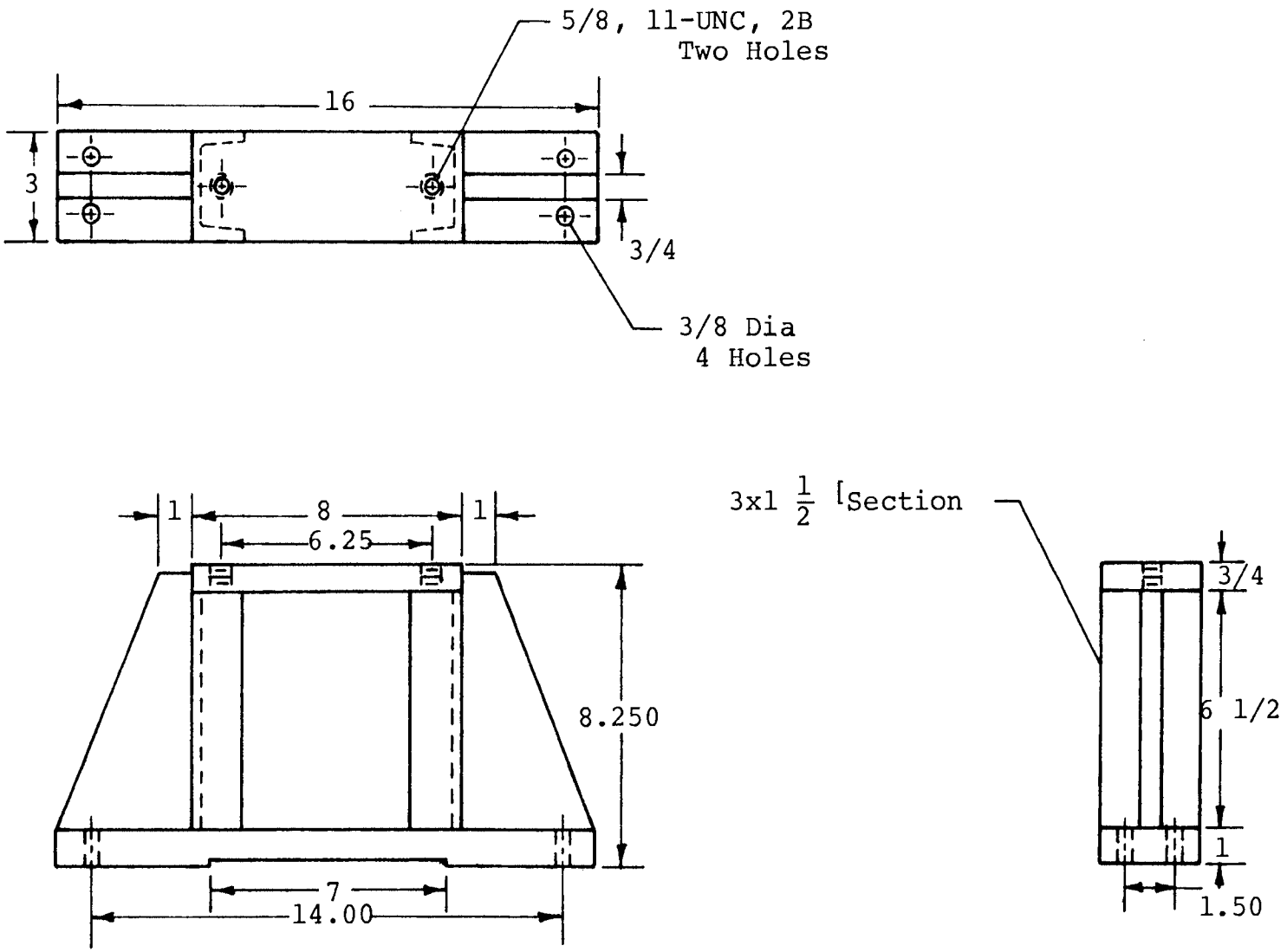

Fig. 2.18. Drive Shaft Bearing Support (Type 2)

G. Pivot Design

Included in the design objective was the desired ability to change the included angle of the Hooke's joint during testing. To allow this the drive assembly is to be hinged, retaining the center of pivot exactly below the center of the Hooke's joint. Due to manufacturing and assembling difficulties this can most easily be achieved by allowing for adjustment within the pivot block.

The pivot design as shown in Fig. 2-19 allows the adjustment of the center of the Hooke's joint along the longitudinal axis. Rectangular holes in pivot plate D allow the longitudinal adjustment required of the drive plate C. A Hooke's joint with splined ends would be used to permit the adjustment of the center along the longitudinal axis. The pivot plate D has a steel bushing, press fitted to it, to provide a normal sliding fit between the pivot pin H and the plate D. After adjusting the center, screws G are tightened. Thus, the drive plate C is rigidly fastened to the pivot plate D. It should be noted that the center, in this specific design, cannot be adjusted perpendicular to the longitudinal axis. For this reason, all dimensions perpendicular to the longitudinal axis should be indicated with as close tolerances as possible. Thus, after adjusting along the longitudinal

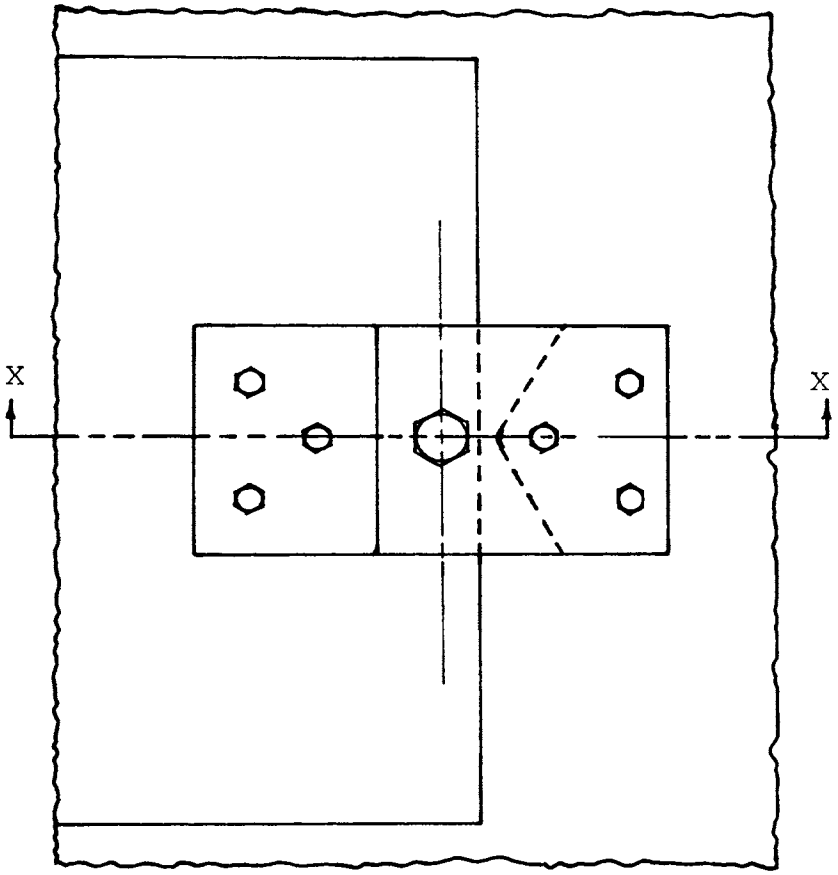

Top View

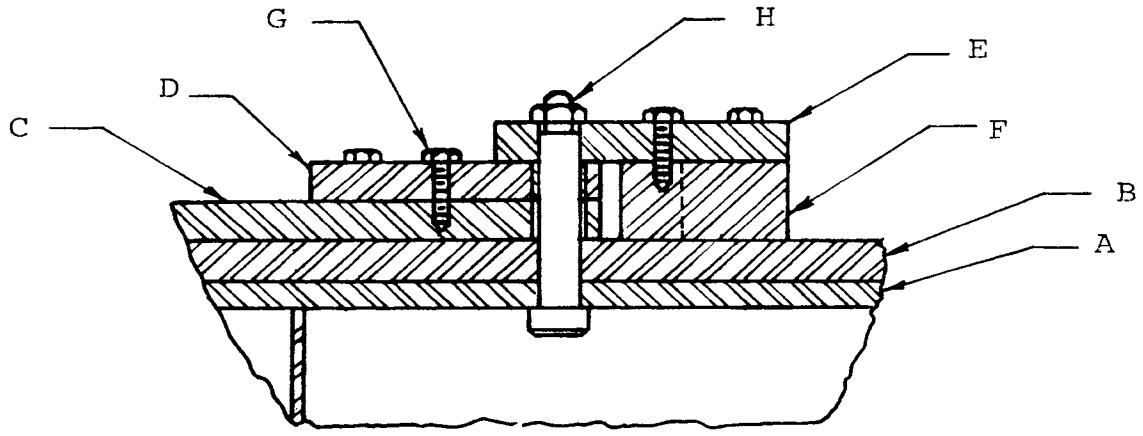

Elevation (section X-X)

Fig. 2.19 Pivot

In Fig. 2.19,

A	Surface Plate Structure
B	Base Plate
C	Drive Plate
D	Pivot Plate 1
E	Pivot Plate 2
F	Pivot Block
G	Pivot Screws
H	Pivot Pin

axis, the center can be obtained below the center of the Hooke's joint within close tolerances.

H. Drive Plate Sliding Mechanism

The power source, flywheel, supporting structure for the flywheel etc. are supported on a plate, called the drive plate which rests on the base of the machine. One end of the drive plate is pivoted to provide the facility of rotating the drive plate in the horizontal plane. Thus, tests can be carried out at different angles of the Hooke's joint, i.e., at different amplitudes of vibration at the specimen. A mechanism is required to rotate the drive plate about the pivot point. This device should require small forces and allow small advancements.

Figure 2.20 shows an arrangement of the mechanism which incorporates a power screw (Acme screw with double thread). Approximately 25 lb-in torque[3] is required to turn the screw, which can be applied easily through a hand crank or an hand wheel. A vernier scale is used to measure the angle.

Locking elements are used to position the drive assembly at a specified angle during testing. Out of four elements, at least two elements are available for any position of the drive assembly. Thus, the drive assembly can be positioned at any angle between and including $\pm 20^{o}$.

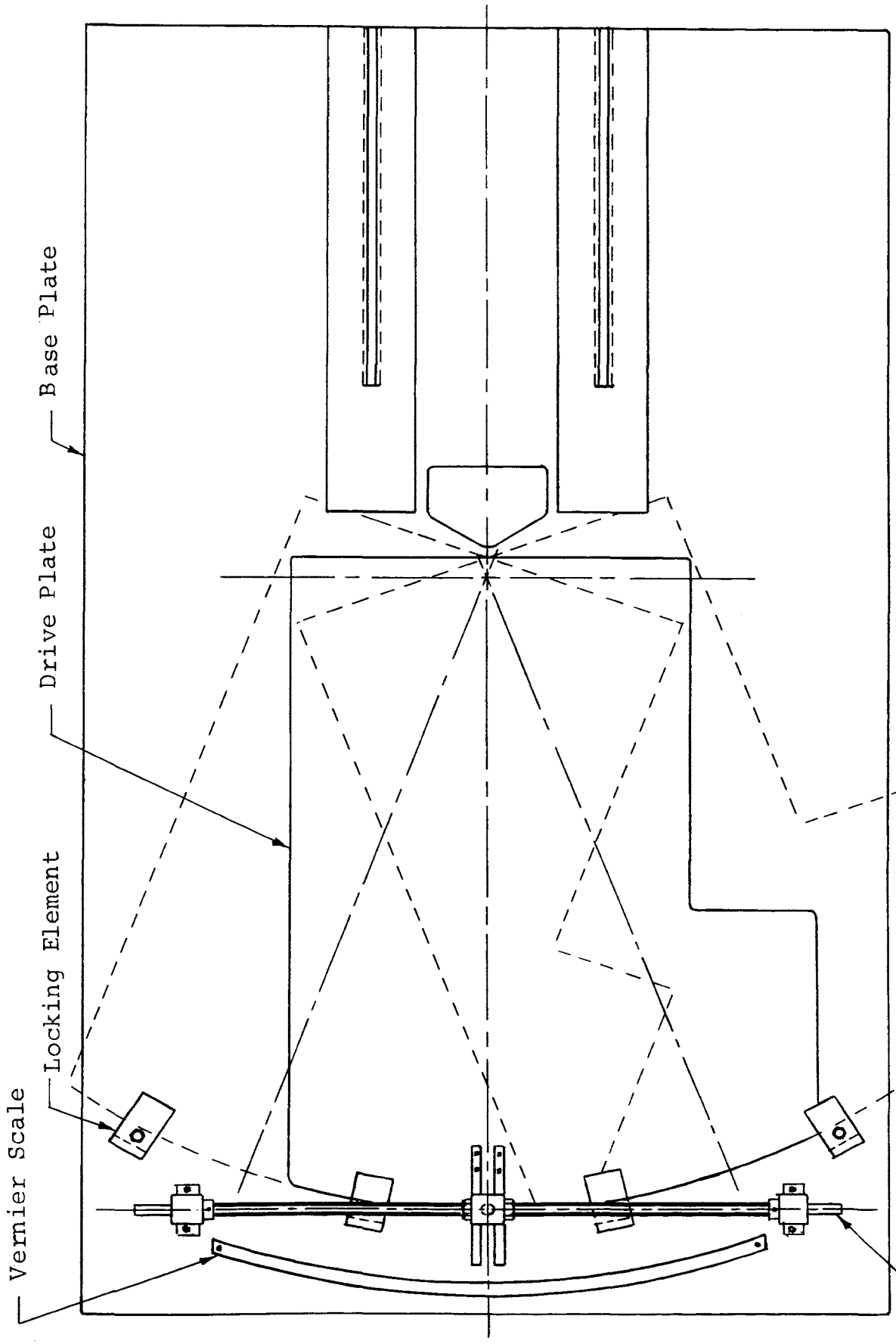

Fig. 2.20 Drive Plate Sliding Mechanism

CHAPTER III
DRIVEN ASSEMBLY

The driven side of the machine consists of the driven shaft, driven shaft bearing, a test item, and support structures for the bearings. Selection of the bearings and the design of the bearing supports for the specimen depend on the type of specimen being tested. The selection and design for a specimen selected by Ashar[2] is considered herein. Two steel blocks with T-slots rigidly attached to the machine base provide the test bed for specimens. T-slots are used to position the specimen bearings at convenient locations. Figure 3.1 shows an elevation view of the driven side assembly.

A. Driven Shaft Bearing and Support Structure

The driven shaft is supported in two bearings mounted on a single support. The bearings were selected to be the same as those on the drive side. Two bearings are required to resist the bending moment on the driven shaft. This bending moment is induced when the input shaft and output shaft of the Hooke's joint are not in a straight line. Figure 3.2 shows two views of the support structure. The longitudinal and transverse spring stiffnesses of the support are calculated to be 13.52×10^6 lb/in and 46.8×10^6 lb/in , respectively. This support

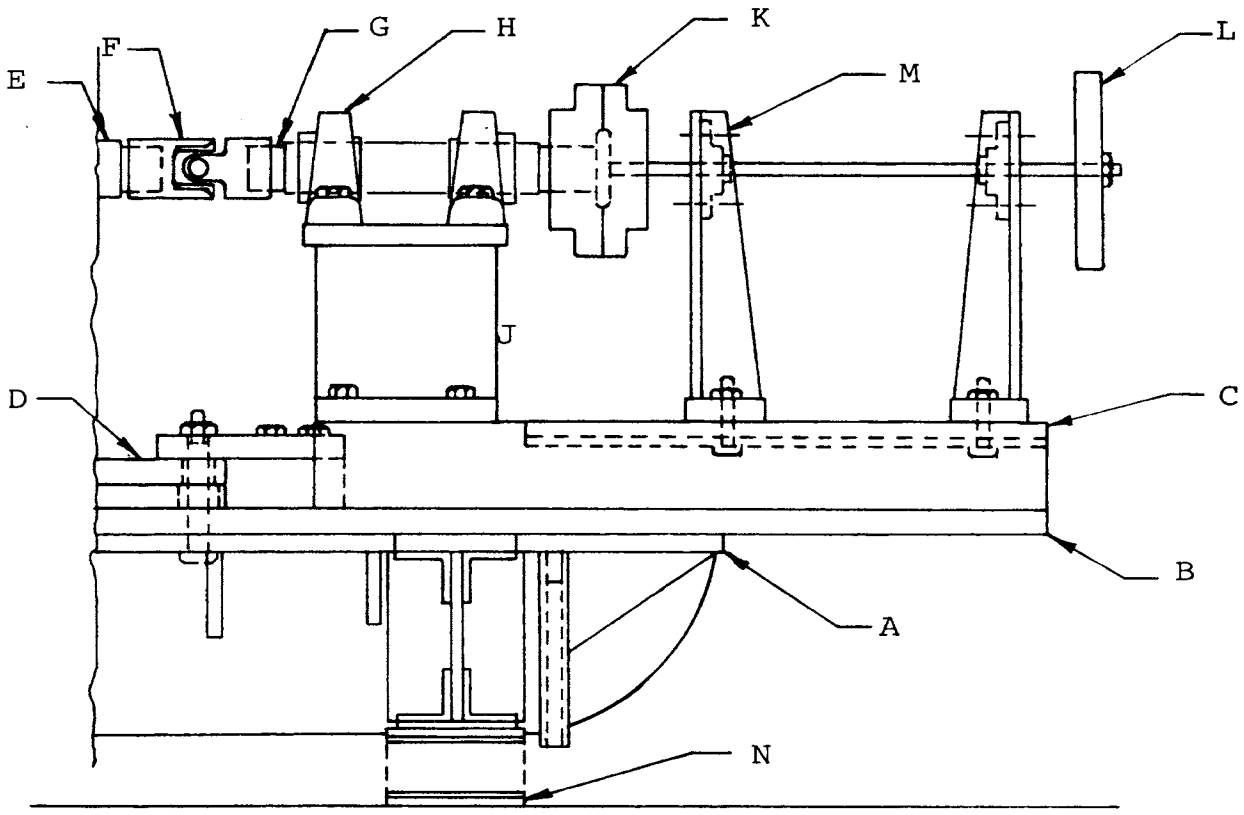

Fig. 3.1. Elevation View of the Driven Side

In Fig. 3.1,

A Surface Plate Structure

B Base Plate

C Test Bed

D Pivot Assembly

E Drive Shaft

F Hooke's Joint

G Driven Shaft

H Driven Shaft Bearing

J Driven Shaft Bearing Support

K Rigid Coupling

L Specimen

M Specimen Bearing Support

N Machine Mounting

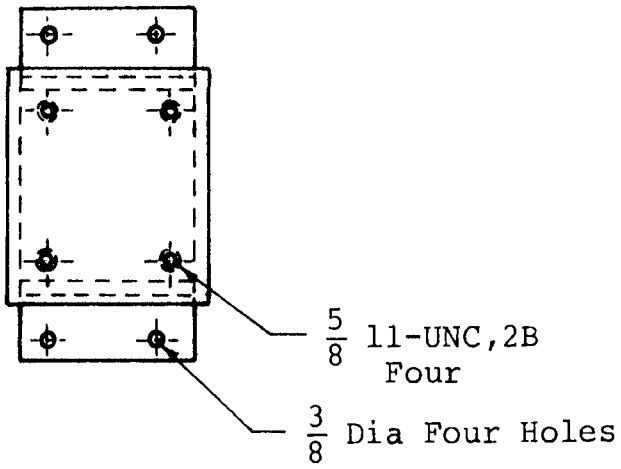

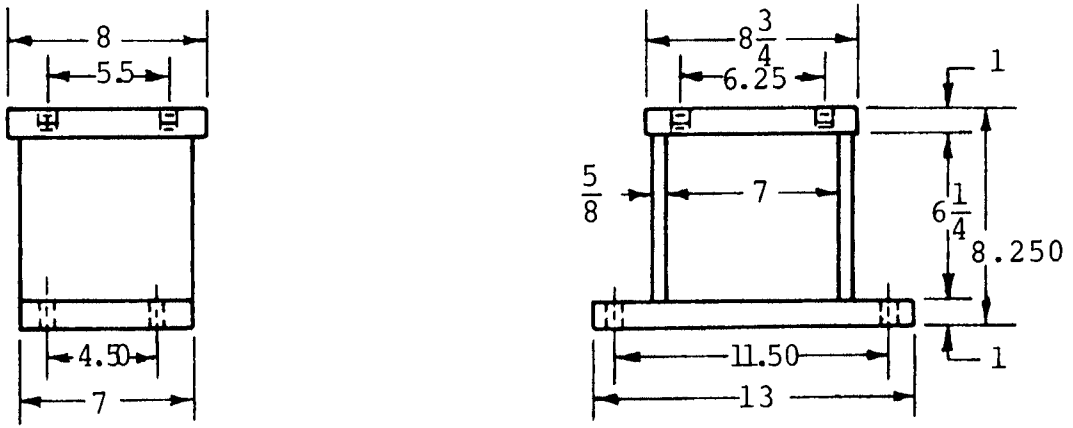

Material-Steel Fig. 3.2 Driven Shaft Bearing Support Scale- 1:8

structure is four times stiffer in longitudinal and 1.7 times stiffer in the transverse direction than the drive shaft bearing support structure. Hence, it is concluded that the driven shaft-support structure assembly meets the stiffness criterion which is derived from the frequency criterion being used for the design.

B. Specimen Bearings and the Support Structure

Figure 3.3 shows the type of specimen considered by Ashar [2] which was selected for further analysis.

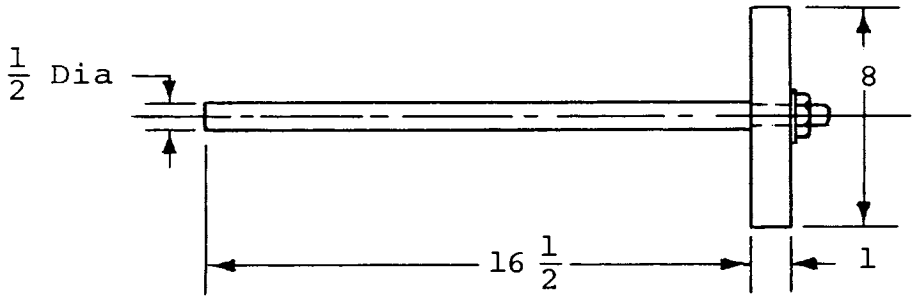

Fig. 3.3 Specimen

Two bearing support designs were considered and are shown in Fig. 3.4 and 3.5. Both designs were analyzed to determine the fundamental vibration characteristics. An isometric view of the system considered for the vibration analysis is shown in Fig. 3.6. The system includes the specimen, bearings, supports, and a rigid coupling. The system is analyzed for uncoupled vibration

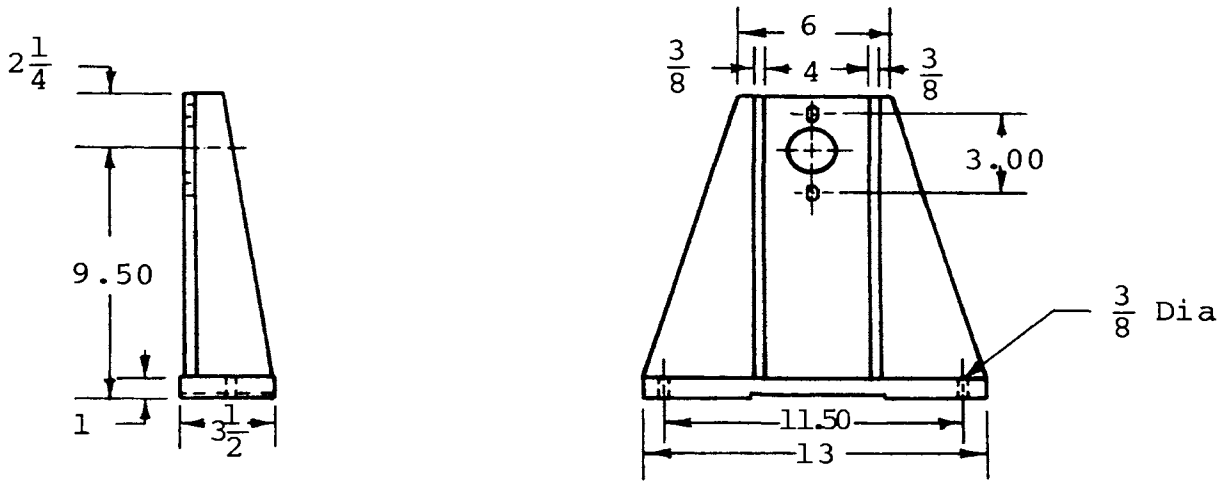

Fig. 3.4 Specimen Bearing Support (Type 1)

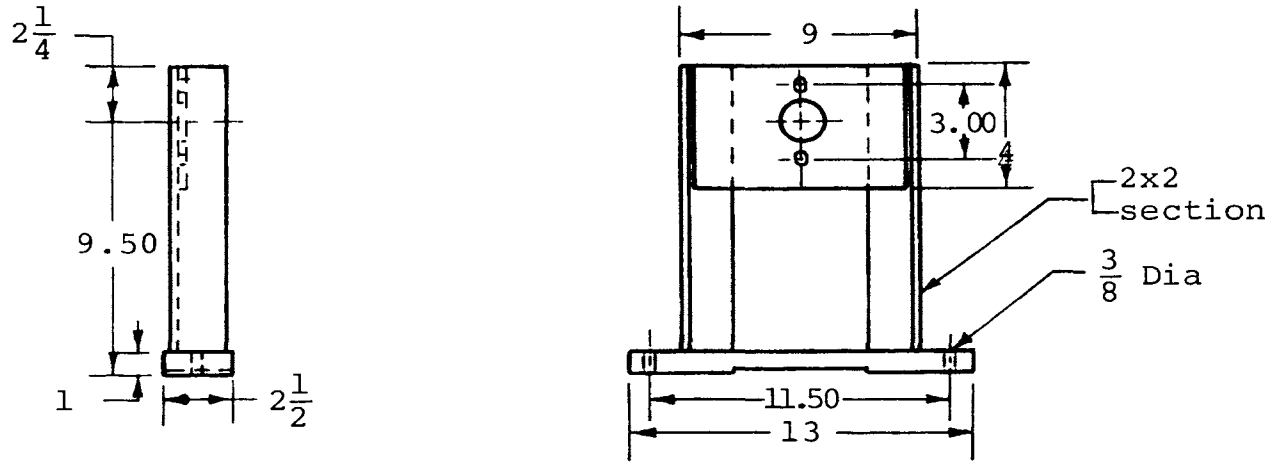

Fig. 3.5 Specimen Bearing Support (Type 2)

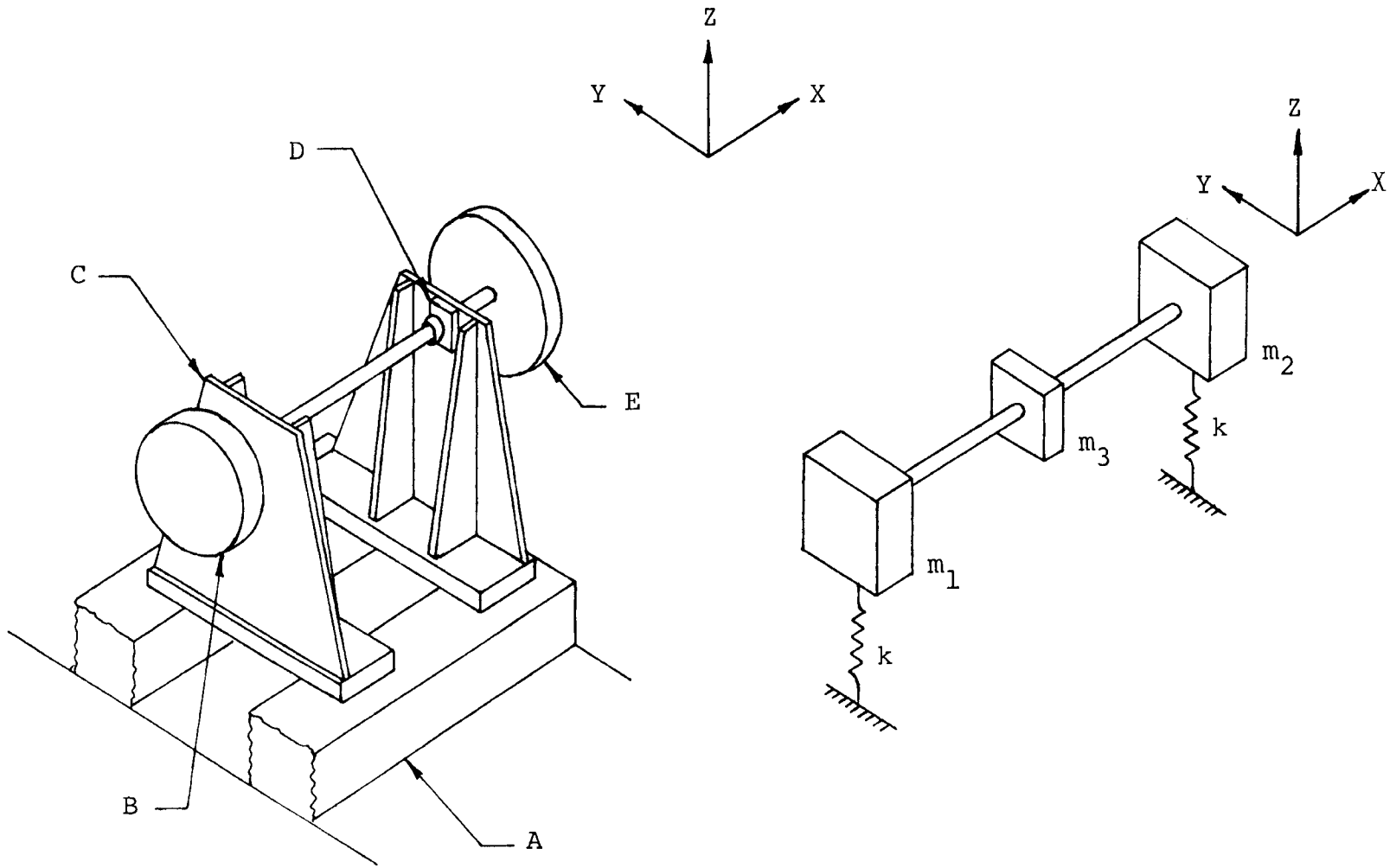

Fig. 3.6. Driven Side Vibration System

In Fig. 3.6,

A	Steel Block with T-slot
B	Rigid Coupling
C	Specimen Bearing Support
D	Specimen Bearing
E	Specimen Disc
k	Spring Stiffness of the Bearing Support
m_1	1/3 weight of the bearing support + 1/3 weight of the specimen shaft + 1/2 weight of the rigid coupling + weight of the bearing
m_2	1/3 weight of the bearing support + 1/3 weight of the specimen shaft + weight of the bearing + weight of the specimen disc
m_3	1/3 weight of the specimen shaft

deflection modes in rocking (longitudinal and transverse) and torsion, as these would be the predominant modes when the specimen is excited by torsional vibrations. For each mode, the actual system was converted into an equivalent discrete spring-mass model system, assuming the specimen to be rigid, and frequencies were calculated for these simplified models of the system. Dunkerley's equation was used to find the approximate fundamental frequency of the system.

1. Longitudinal Rocking Mode

The discrete spring-mass model and the respective deflection mode is shown in Fig. 3.7. Approximate natural frequency of this simplified model of the system is given by:

$$f_1 = \frac{1}{2\pi} \sqrt{\frac{2k_1 g}{m_1+m_2+m_3}} \qquad (3.1)$$

where:

f_1 = Natural frequency of vibration of the system in longitudinal rocking mode, cps

k_1 = Longitudinal spring stiffness of the bearing support, lb/in

m_1 = 1/3 weight of the bearing support + 1/3 weight of the specimen shaft + weight of the bearing + 1/2 weight of the coupling, lbs

m_2 = 1/3 weight of the bearing support + 1/3 weight of the specimen shaft + weight of the bearing + weight of the specimen disc, lbs

m_3 = 1/3 weight of the specimen shaft

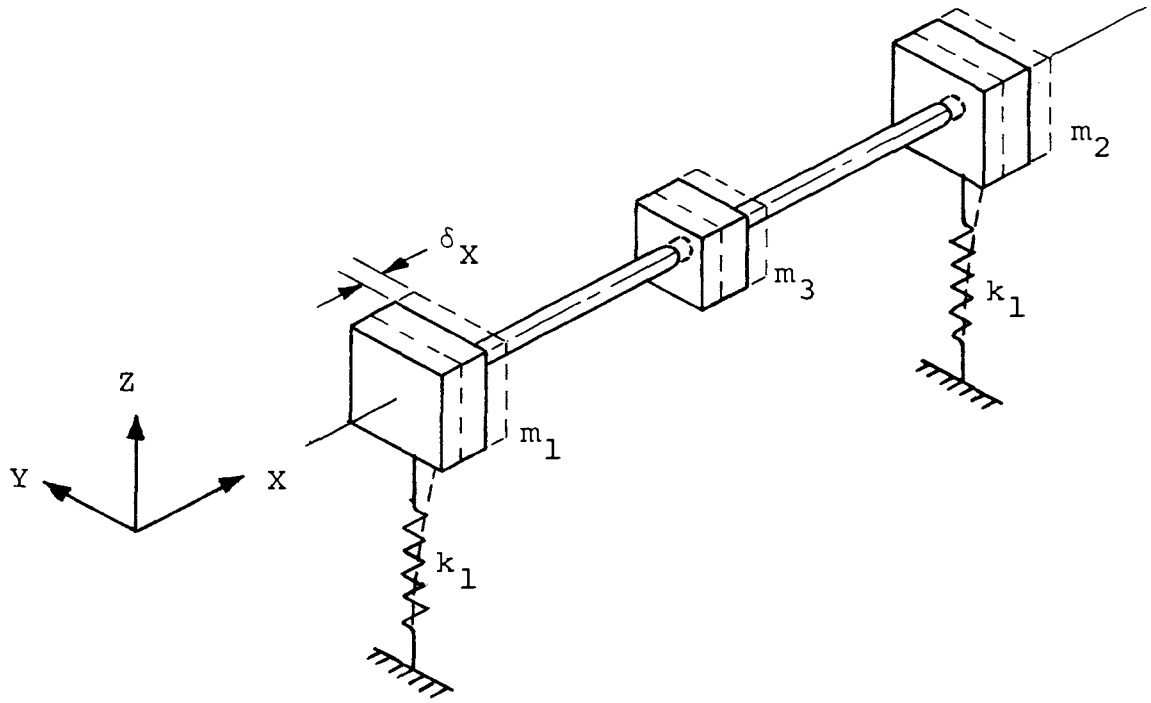

k_1 - Longitudinal spring stiffness of the bearing support

m_1 - 1/3 weight of the bearing support + 1/3 weight of the specimen shaft + weight of the bearing + 1/2 weight of the coupling

m_2 - 1/3 weight of the bearing support + 1/3 weight of the specimen shaft + weight of the bearing + weight of the specimen disc

m_3 - 1/3 weight of the specimen shaft

δ_X - Deflection in X-direction

Fig. 3.7 Longitudinal Rocking Mode

The spring stiffness, k_1, is calculated by treating the support as cantilever beam and using average cross sectional properties of the support. Substituting k_1 = 0.221 x 10^6 lb/in, m_1 = 18.0 lbs., m_2 = 20 lbs and m_3 = 0.3 lbs into Eq. (3.1), gives:

$$f_1 = \frac{1}{2\pi}\sqrt{\frac{2x0.221x10^6x386}{(18+20+.3)}} = 336 \text{ cps}$$

2. Transverse Rocking Mode

In this mode the major deflections are in the Y-direction as shown in Fig. 3.8. The approximate natural frequency for this mode is given by:

$$f_2 = \frac{1}{2\pi}\sqrt{\frac{2k_2g}{m_1+m_2+m_3}} \qquad (3.2)$$

where:

f_2 = Natural frequency of vibration of the system in transverse rocking mode, cps

k_2 = Transverse spring stiffness of the support, lb/in.

Substituting k_2 = 3.575 x 10^6 lb/in., m_1 = 18.0 lbs., m_2 = 20 lbs., and m_3 = 0.3 lbs into Eq. (3.2), gives:

$$f_2 = \frac{1}{2\pi}\sqrt{\frac{2x3.575x10^6x386}{(18+20+0.3)}} = 1350 \text{ cps}$$

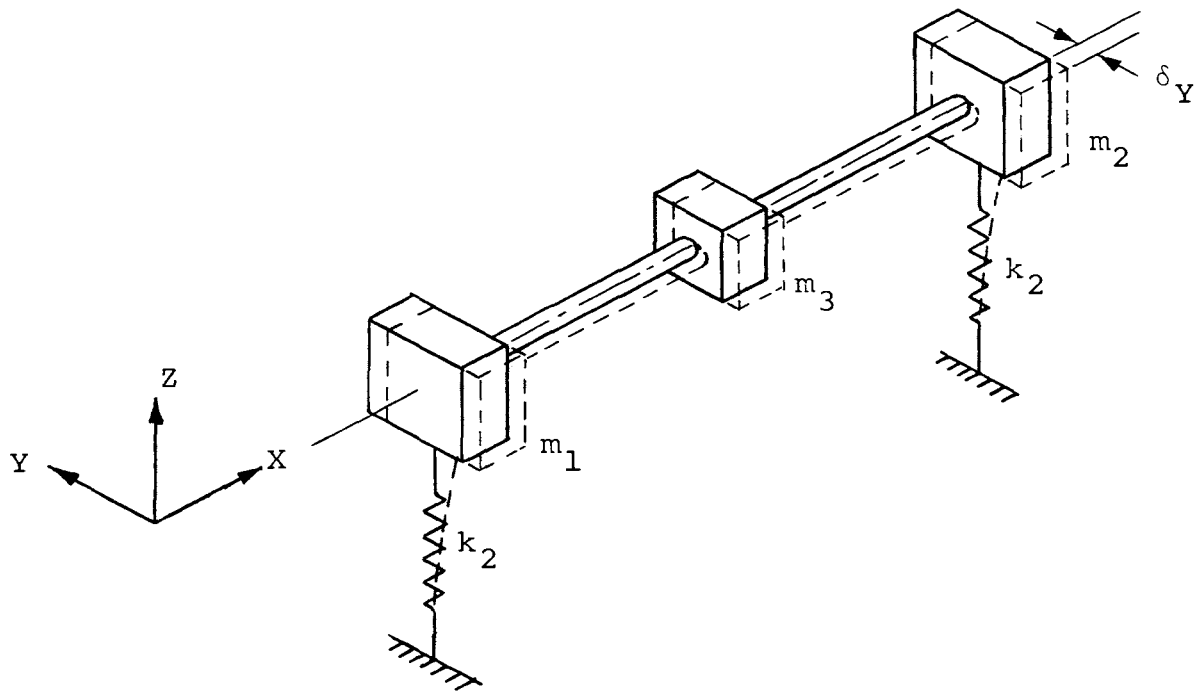

k_2 - Transverse spring stiffness of the bearing support

m_1 - 1/3 weight of the bearing support + 1/3 weight of the specimen shaft + weight of the bearing + 1/2 weight of the coupling

m_2 - 1/3 weight of the bearing support + 1/3 weight of the specimen shaft + weight of the bearing + weight of the specimen disc

m_3 - 1/3 weight of the specimen shaft

δ_Y - Deflection in Y-direction

Fig. 3.8 Transverse Rocking Mode

3. Torsional Mode

In this mode the system may rotate in the XY-plane as shown in Fig. 3.9. The approximate natural frequency for this mode is given by:

$$f_3 = \frac{1}{2\pi}\sqrt{\frac{2k_3 l^2}{I + \frac{m_1'}{g} l^2 + \frac{m_2'}{g} l^2}} \qquad (3.3)$$

where:

f_3 = Natural frequency of vibration of the system in torsional mode, cps

$k_3 = k_2$ = Transverse spring stiffness of the bearing support, lb/in.

I = Mass moment of inertia of the specimen shaft about the axis at its mid length, lb-in-sec^2.

m_1' = 1/3 weight of the support + weight of the bearing + 1/2 weight of the coupling, lbs.

m_2' = 1/3 weight of the support + weight of the bearing + weight of the specimen disc, lbs.

Substituting $k_3 = 3.57 \times 10^6$ lb/in., $I = 0.044$ lb-in-sec^2, $m_1 = 17.70$ lbs., $m_2 = 19.80$ lbs. and $l = 5.38$ in. into Eq. (3.3), gives:

$$f_3 = \frac{1}{2\pi}\sqrt{\frac{2\times 3.575\times 10^6 \times 5.38^2}{0.044+(17.70/386+19.80/386)5.38^2}} = 1350 \text{ cps}$$

The approximate fundamental frequency, f, calculated by using Dunkerley's equation is 316 cps.

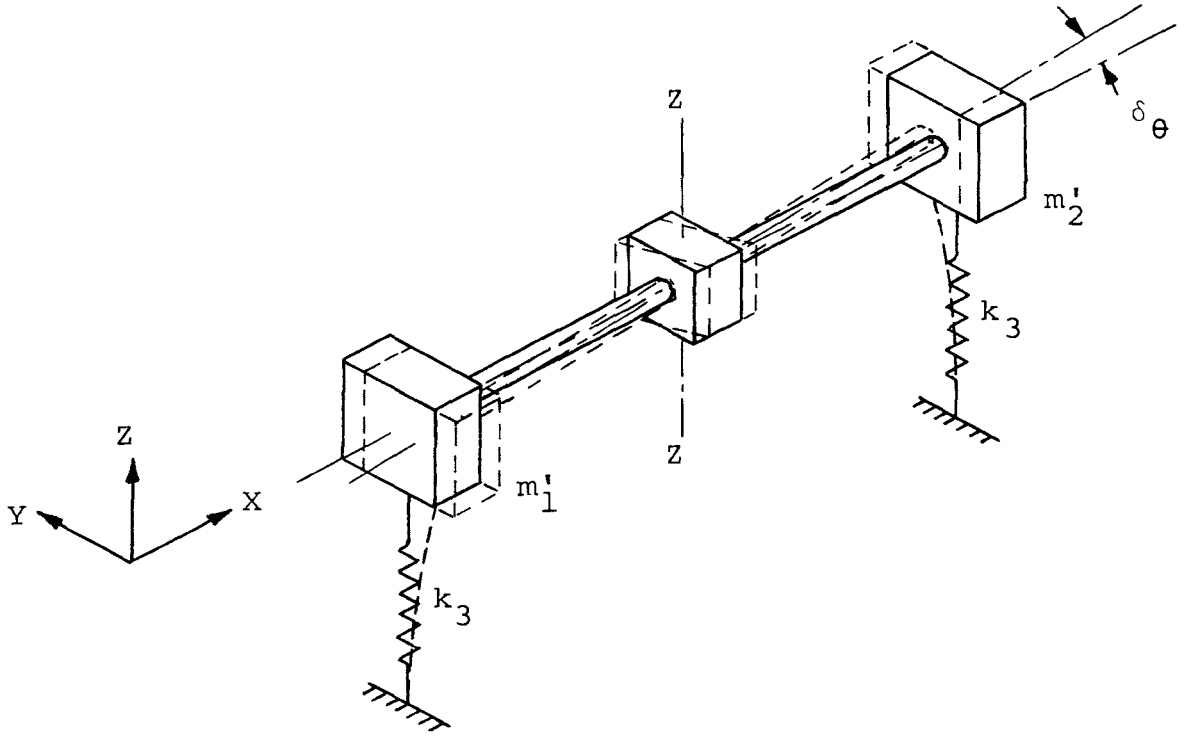

k_3 - Transverse spring stiffness of the bearing support

m_1' - 1/3 weight of the support + weight of the bearing + 1/2 weight of the coupling

m_2' - 1/3 weight of the support + weight of the bearing + weight of the specimen disc

δ_θ - Rotation of the system in X-Y plane about Z-axis

Fig. 3.9 Torsional Mode

The vibration analysis of the system with the second type of support as shown in Fig. 3.5 reveals the following frequencies. Natural frequency of vibration in

1. Longitudinal rocking mode - 192 cps
2. Transverse rocking mode - 1242 cps
3. Torsional mode - 1222 cps
4. Fundamental frequency of the support-structure system - 182 cps

The comparison of results shows that the first type of support is stiffer than the second and, hence, should be selected.

CHAPTER IV
DESIGN OF BASE AND MACHINE MOUNTINGS

A heavy and wide base structure is required to support the drive and driven assemblies. While specifying the criteria for a base of proper size and stiffness for the machine, a surplus surface plate structure, as shown in Fig. 4.1, became available and was considered appropriate for this application. The machine base is shown in Fig. 4.2. It consists of the surface plate structure, a base plate of aluminum or steel of 72 x 40 x 1 inches, two steel blocks with T-slots and four machine mountings to provide support for vibration pads. Each steel block is 28 x 4 1/2 x 3 1/2 inches and has a 3/8 T-slot. The steel blocks are rigidly fastened to the base plate, which is rigidly connected to the surface plate structure.

The upper surface of the base plate on the drive side will have to be machined with a close surface tolerance as it supports the drive assembly which is to be rotated in the horizontal plate and set at different angles of the Hooke's joint. Also, the upper surface of the steel blocks, which support the driven shaft bearing and specimen bearing support structures, will have to be machined with a close surface tolerance. The machined surface should be completed at one set-up, since it serves as the reference surface for all perpendicular measurements.

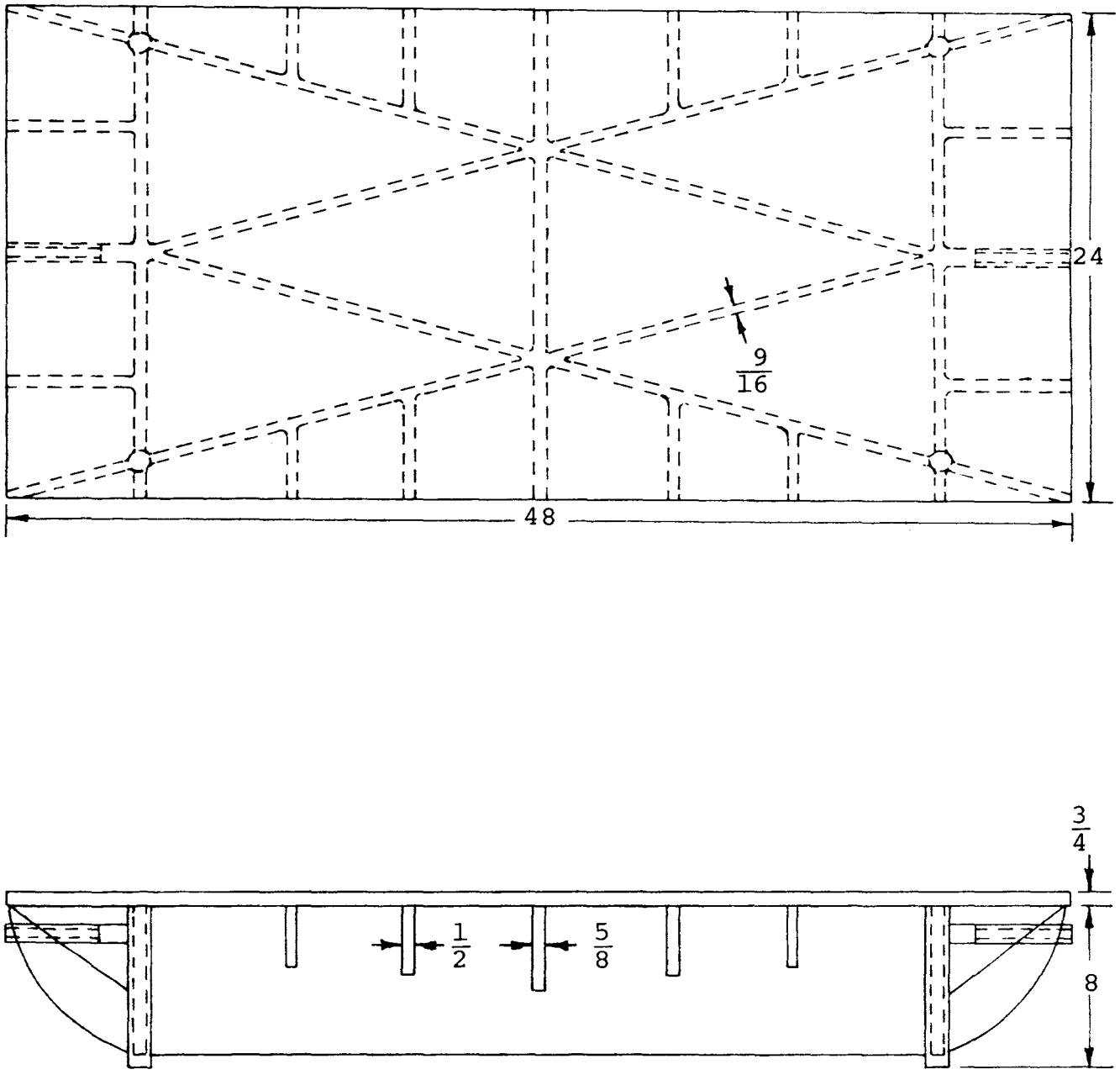

Fig. 4.1 Cast Steel Surface Plate Structure

A Base Plate

B Machine Mounting

C Surface Plate Structure

D Steel Block with T-Slot

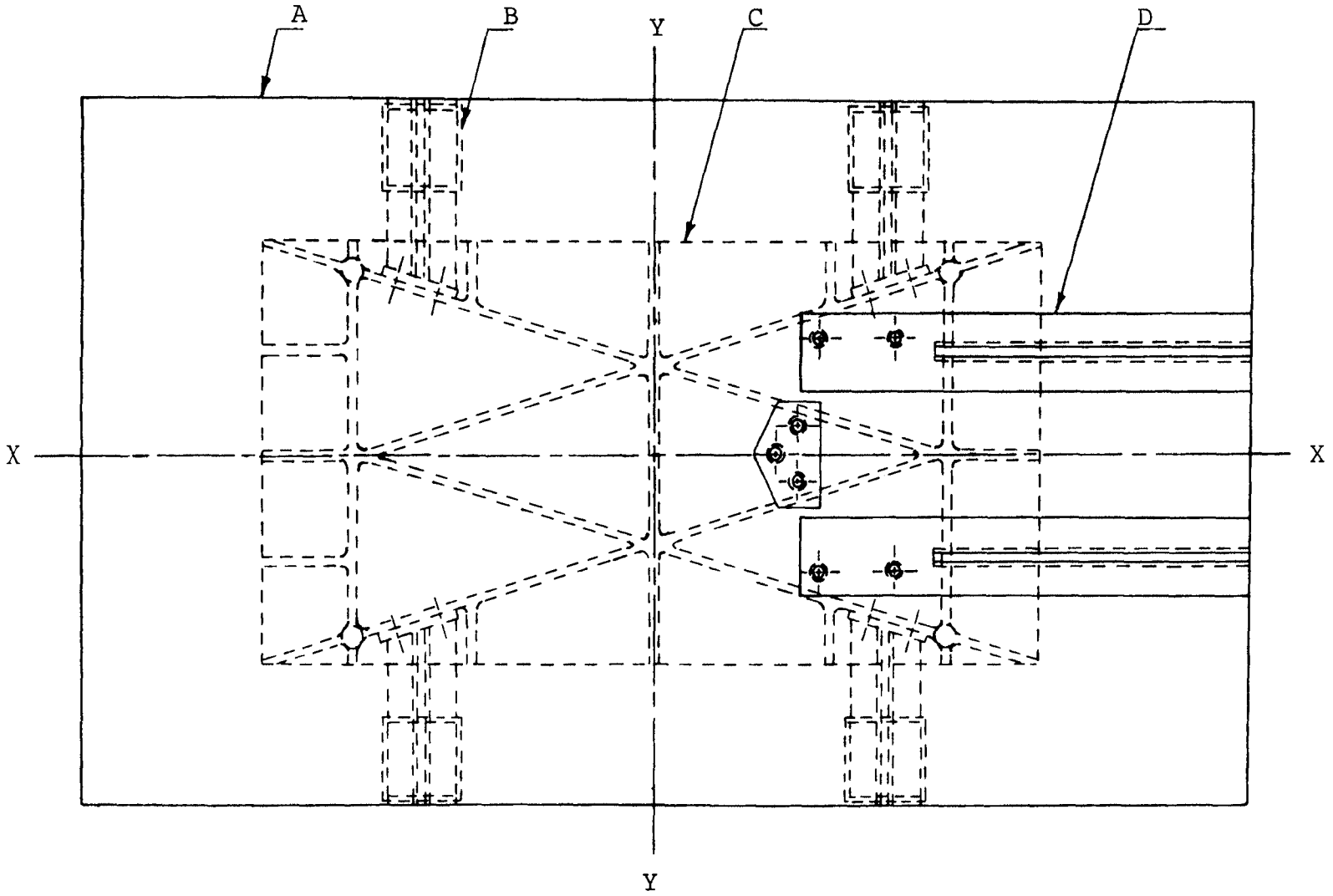

Fig. 4.2 Machine Base

The machine is supported on vibration pads which are selected such that the fundamental frequency of the pad-machine system is below 7 cps. This ensures that the ratio of the lowest forcing frequency applied during testing and the fundamental frequency will be above 1.4, i.e., transmissibility is less than one. The details of the machine mounting are given in Fig. 4.3.

A. Machine Mountings

Figures 4.2 and 4.3 show the location and details of each mounting, respectively. The natural frequencies of vertical and torsional vibration modes of the system, consisting of the machine, four legs and five pads under each leg were calculated. For these calculations the machine was assumed to be a rigid mass. Dunkereley's equation was used to find the approximate fundamental natural frequency of the system.

The total approximate weight of the machine is calculated to be 2300 lbs. Assuming equal loading, each leg would carry 575 lbs. From the load deflection curve of an isomode pad [9], the linearized spring stiffness in the vicinity of a 30 psi static equilibrium position is 1000 $lb/in^2/in$. The area required to have a 30 psi loading on the pad is 19.166 in^2. Therefore,

k_p = Stiffness of each pad = 19.166x1000 = 19166 lb/in.

k_{pe} = Equilvalent spring stiffness of five pads

$$= \frac{19166}{5} = 3830 \text{ lb/in}$$

The natural frequency of vertical vibration is given by:

$$f_v = \frac{1}{2\pi} \sqrt{\frac{4k_{pe} \times 386}{M_t}} \qquad (4.1)$$

where:

M_t = Total weight of the machine

Substituting k_{pe} = 3830 lb/in and M_t = 2300 lbs. into Eq. (4.1), gives:

$$f_v = \frac{1}{2\pi} \sqrt{\frac{4x3830x386}{2300}} = 8.07 \text{ cps}$$

The natural frequencies of torsional vibrations about the X-axis, Y-axis and Z-axis (see figure 4.2) are given by:

$$f_{tx} = \frac{1}{2\pi} \sqrt{\frac{4k_{pe}(\frac{L_1}{2})^2}{J_k}} \qquad (4.2)$$

$$f_{ty} = \frac{1}{2\pi} \sqrt{\frac{4k_{pe}(\frac{L_2}{2})^2}{J_y}} \qquad (4.3)$$

$$f_{tz} = \frac{1}{2\pi} \sqrt{\frac{4k_{se}(\frac{L_2}{2})^2}{J_z}} \qquad (4.4)$$

where:

L_1 = c/c distance between pads along Y-axis, in.

J_x = Mass moment of inertia of the machine about X-axis, lb-in-sec^2

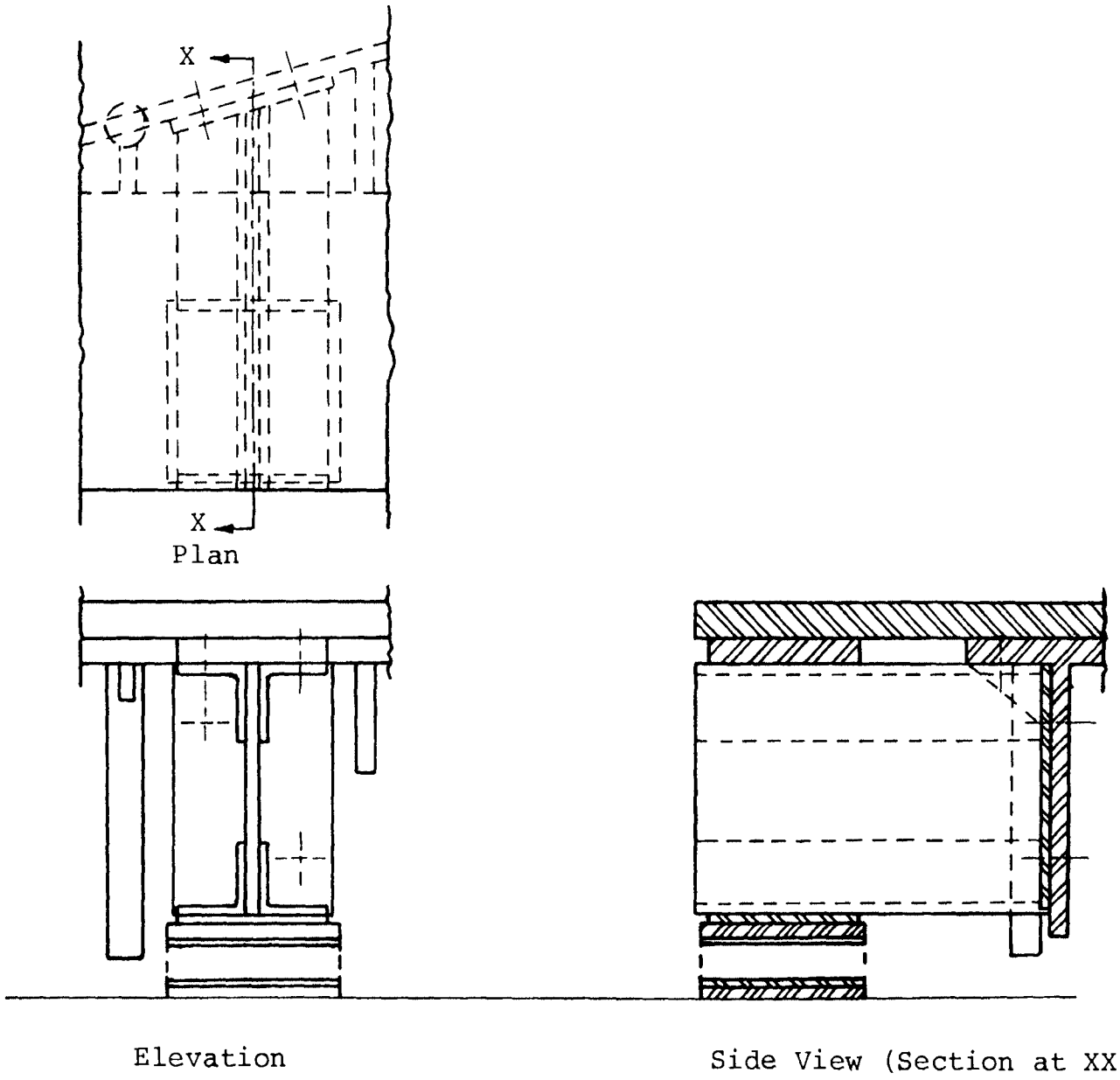

Fig. 4.3. Details of the Mounting

L_2 = c/c distance between pads along X-axis, in.

J_y = Mass moment of inertia of the machine about Y-axis, lb-in-sec^2.

k_{se} = Equivalent spring stiffness of five pads in shear, lb/in.

J_z = Mass moment of inertia of the machine about Z-axis, lb-in-sec^2

The mass moment of inertias J_x, J_y and J_z of the machine were calculated approximately. Only the heavier members (base, base plate, drive plate and flywheel) were considered in these calculations. Substituting L_1 = 34.63 in., J_x = 425 lb-in-sec^2, L_2 = 29 in., J_y = 875 lb-in-sec^2, k_{se} = 1000 lb/in., J_z = 1300 lb-in-sec^2 into Eq. (4.2), (4.3) and (4.4), gives:

$$f_{tx} = \frac{1}{2\pi}\sqrt{\frac{4\times3830\times(\frac{34.63}{2})^2}{425}} = 16.5 \text{ cps}$$

$$f_{ty} = \frac{1}{2\pi}\sqrt{\frac{4\times3830\times(\frac{29}{2})^2}{875}} = 9.65 \text{ cps}$$

$$f_{tz} = \frac{1}{2\pi}\sqrt{\frac{4\times1000\times(\frac{29}{2})^2}{1300}} = 4 \text{ cps}$$

The effectiveness of the isolating system is examined for each mode by transmissibility equation given by:[8]

$$TR = \frac{1}{(f/f_n)^2 - 1} \qquad (4.5)$$

where:

TR = Transmissibility

f = Lowest excitation frequency, cps.

f_n = Natural frequency of the pads-machine system for each mode, cps.

Due to damping in the pads, the actual transmissibility is higher than the calculated values. It is also known that vibration isolation is possible only for $f/f_n > \sqrt{2}$. Thus, it is noted that, in this specific design, vibration isolation is not possible for torsional vibrations about the X-axis and Y-axis. Substituting f = 12 cps, $f_n = f_v$ = 8.07 cps and $f_n = f_{tz}$ = 4 cps into Eq. (4.5), gives:

$$TR = \frac{1}{(\frac{12}{8.07})^2 - 1} = 0.91 \text{ (vertical vibrations)}$$

$$TR = \frac{1}{(\frac{12}{4})^2 - 1} = 0.125 \text{ (torsional vibrations about Z-axis)}$$

The fundamental natural frequency of the pads-machine system as calculated by using Dunkereley's equation is 3.3 cps. Substituting this value into Eq. (4.5), gives:

$$TR = \frac{1}{(\frac{12}{3.3})^2 - 1} = 0.087$$

CHAPTER V

CONCLUSIONS

The machine can be manufactured by conventional machining operations. An elevation view, a top view, and details of each member of the machine are given in Appendix A. The dimensions of standard elements such as V-belt sheaves, bearings, Hooke's joint, bolts, etc., were taken from the respective manufacture's catalogue and machinery's hand book.

The expected output of the machine is a constant angular motion with an approximate sinusoidal angular motion superimposed upon it. This type of motion can be used to investigate test models representing crankshafts, gear trains, torsional dampers, etc., for their torsional vibration characteristics including nonlinear effect. The motor has been selected for satisfactory performance for specimens having mass moment of inertias to 0.314 lb-in-sec^2. Higher capacity can be obtained by selecting a higher H.P. motor. However, the range of testing frequency cannot be increased, as all members of the machine have been designed for the range 12-33 cps.

It is recommended that the detail dimensions of the proposed design be thoroughly checked before completing a list of materials and manufacturing any parts. This final step, thus, completes the generally accepted engineering design sequence.

BIBLIOGRAPHY

1. Yada, T., "On Planetary Gear Type Alternating Torque Generator", Bulletin of JSME 9, 1966, 36, 694-7-1.

2. Ashar, N.T., "Dynamic Analysis of a Torsional Vibration Actuator", M.S. Thesis, September 1970, University of Missouri-Rolla.

3. Shigley, Joseph Edward, "Mechanical Engineering Design", McGraw Hill Book Company, Inc., New York, 1963, P. 631.

4. Kent's Mechanical Engineers' Hand Book; Design, Shop Practice, John Wiley and Sons, Inc., 1938.

5. Timoshenko S., "Vibration Problems in Engineering", D. Van Nostrand Company, Inc., 1957, P. 470.

6. C.A. Norman, "High Speed Belt Drives", Bulletin No. 83, May 1934, The Engineering Experiment Station, The Ohio State University.

7. Hagenbook, L.D., and Holstein, J.H., "Universal Joints", Product Engineering, Vol. 13, No. 6, 1942, P. 334-336.

8. William T. Thomson, "Vibration Theory and Applications", Prentice-Hall, Inc., 1965, P. 384.

9. MB Isomode Vibration Pads, Bulletin 630-5M-3-70, MB Electronics, New Haven, Connecticut.

VITA

Prafulchandra Pragjibhai Desai was born on November 3, 1945 in Amalsad, India. He received his primary and secondary education in Baroda, India. He received his college education from the M.S. University, Baroda, India, where he received the degree Bachelor of Engineering in Mechanical Engineering in June 1969.

He has been enrolled as a graduate student in the graduate school of the University of Missouri-Rolla, Rolla, Missouri since January 1970.

APPENDIX A

ASSEMBLY DRAWING AND DETAILS

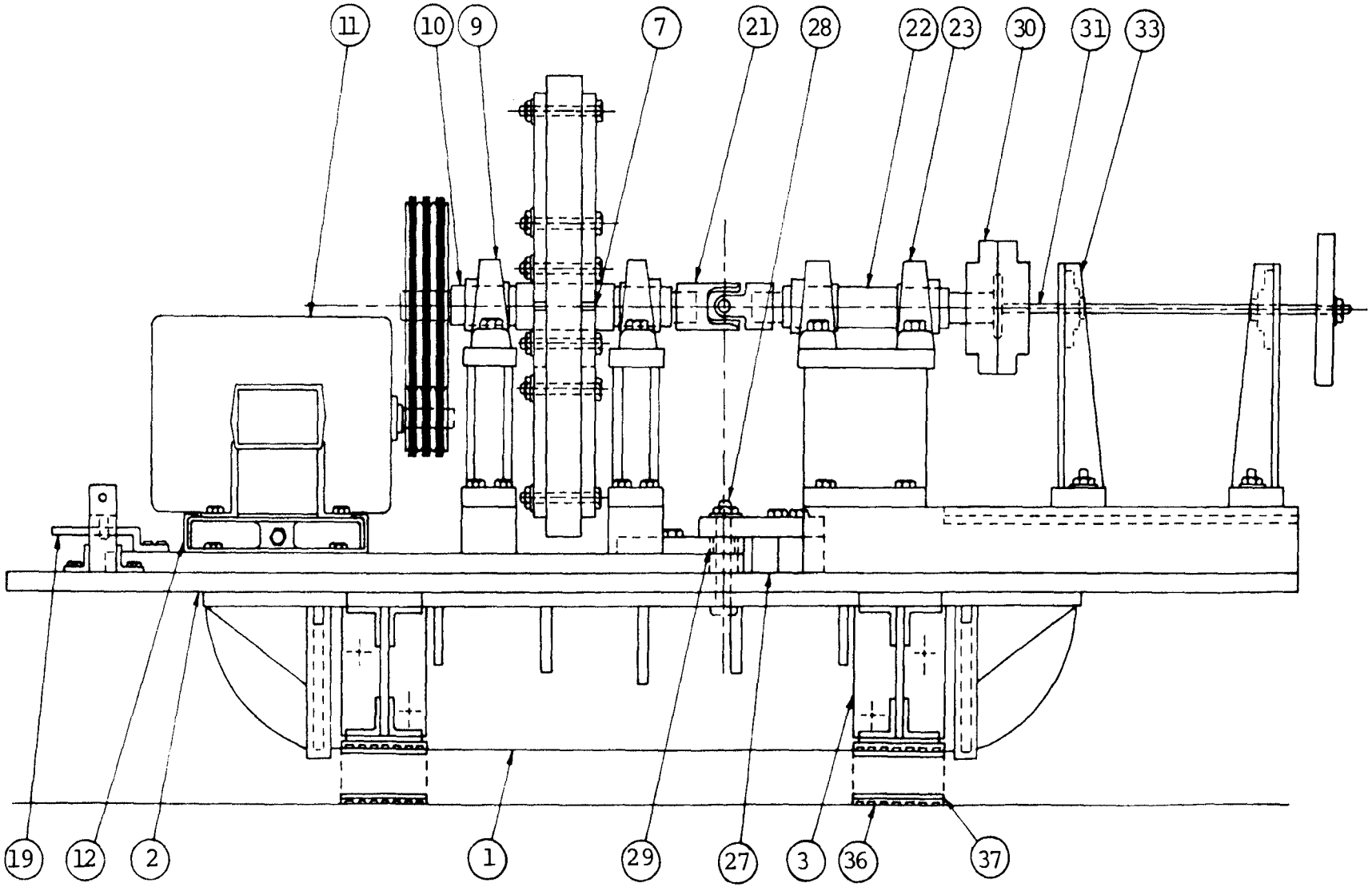

Fig. A.1 Elevation View of the Torsional Vibration Machine

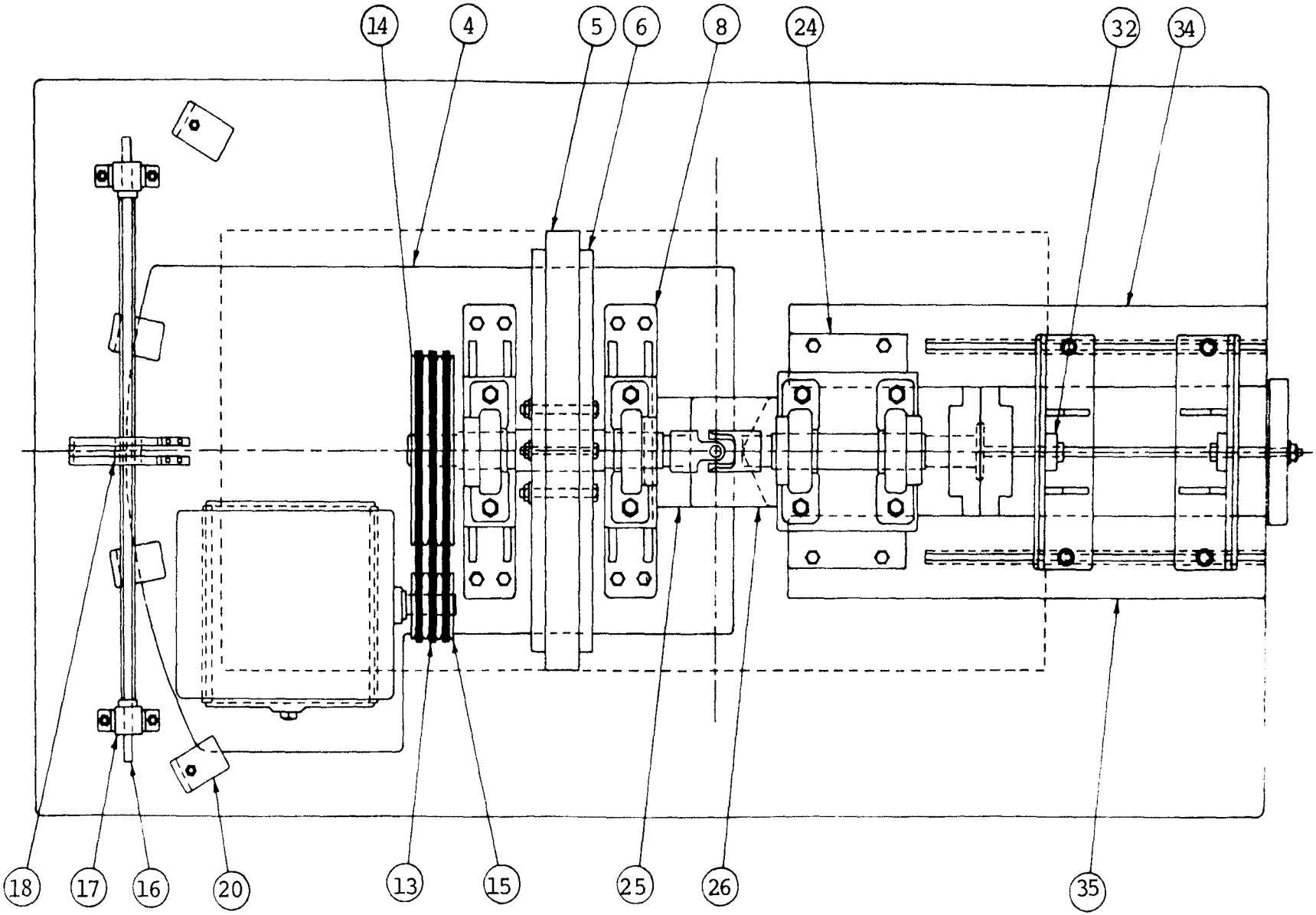

Fig. A.2 Top View of the Torsional Vibration Machine

TABLE III

Description of Items in Fig. A.1 and A.2

ITEM	QUAN	FIG.	DESCRIPTION
1	1	A.3	Surface Plate Structure
2	1	A.4	Base Plate
3	4	A.5	Machine Mounting
4	1	A.6	Drive Plate
5	1	A.7	Flywheel
6	8	A.8	Flywheel Segment
7	2	A.9	Flange
8	2	A.10	Drive Shaft Bearing Support
9	2	PUR	Drive Shaft Bearing
10	1	A.11	Drive Shaft
11	1	PUR	D.C. Shunt Motor
12	1	PUR	Slide Motor Base
13	1	PUR	Small Sheave
14	1	PUR	Large Sheave
15	3	PUR	V-Belt
16	1	A.12	Adjusting Screw
17	2	A.13	Screw Support
18	1	A.14	Nut
19	2	A.15	Guide
20	4	A.16	Locking Element
21	1	PUR	Hooke's Joint
22	1	A.17	Driven Shaft

TABLE III (continued)

ITEM	QUAN	FIG	DESCRIPTION
23	2	PUR	Driven Shaft Bearing
24	1	A.18	Driven Shaft Bearing Support
25	1	A.19	Pivot Plate 1
26	1	A.20	Pivot Plate 2
27	1	A.21	Pivot Block
28	1	PUR	Pivot Pin
29	1	PUR	Pivot Bushing
30	1	PUR	Rigid Coupling
31	1	A.22	Specimen
32	2	PUR	Specimen Bearing
33	2	A.23	Specimen Bearing Support
34	1	A.24	Steel Block 1
35	1	A.25	Steel Block 2
36	20	PUR	Isomode Vibration Pad
37	16	A.26	Pad Plate

Note - All figures have dimensions in inches.

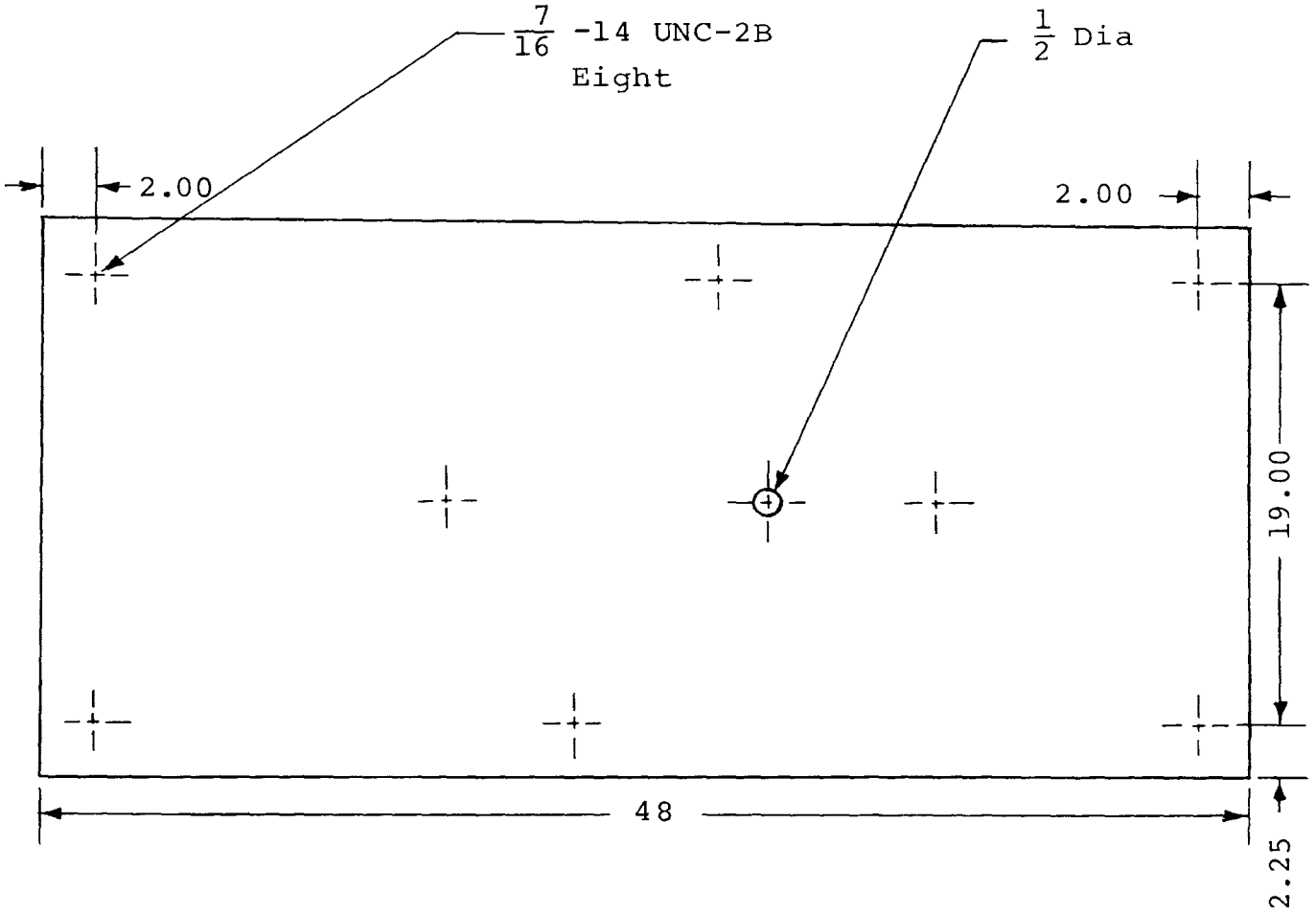

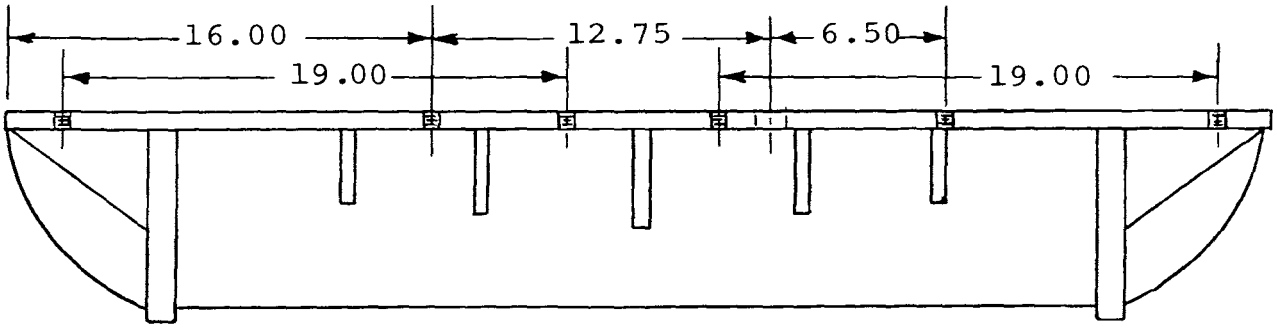

Fig. A.3 Cast Steel Surface Plate Structure

Scale- 1:8

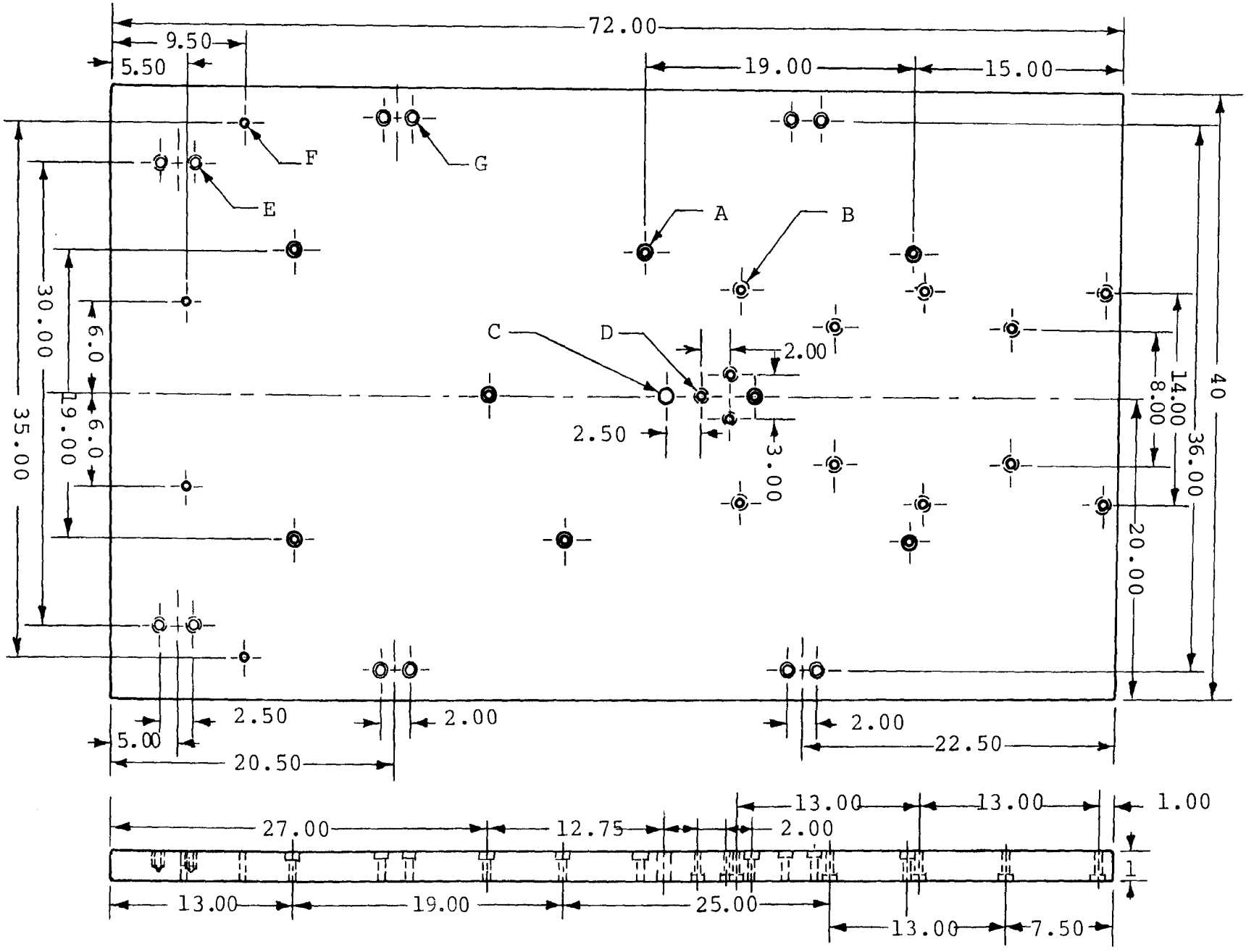

Fig. A.4 Base Plate

Scale- 1:10

In Fig. A.4,

A $\frac{7}{16}$ DIA, $\frac{21}{32}$ CBORE to $\frac{7}{16}$ DEPTH, Eight Holes

B $\frac{7}{16}$ DIA, $\frac{21}{32}$ CBORE to $\frac{7}{16}$ DEPTH, Ten Holes

C 1" DIA

D $\frac{7}{16}$ DIA, $\frac{21}{32}$ CBORE to $\frac{7}{16}$ DEPTH, Three Holes

E $\frac{1}{4}$ -20UNC-2B, Four Holes

F $\frac{1}{4}$ DIA, Four Holes

G $\frac{5}{16}$ DIA, $\frac{15}{32}$ CBORE to $\frac{5}{16}$ DEPTH, Eight Holes

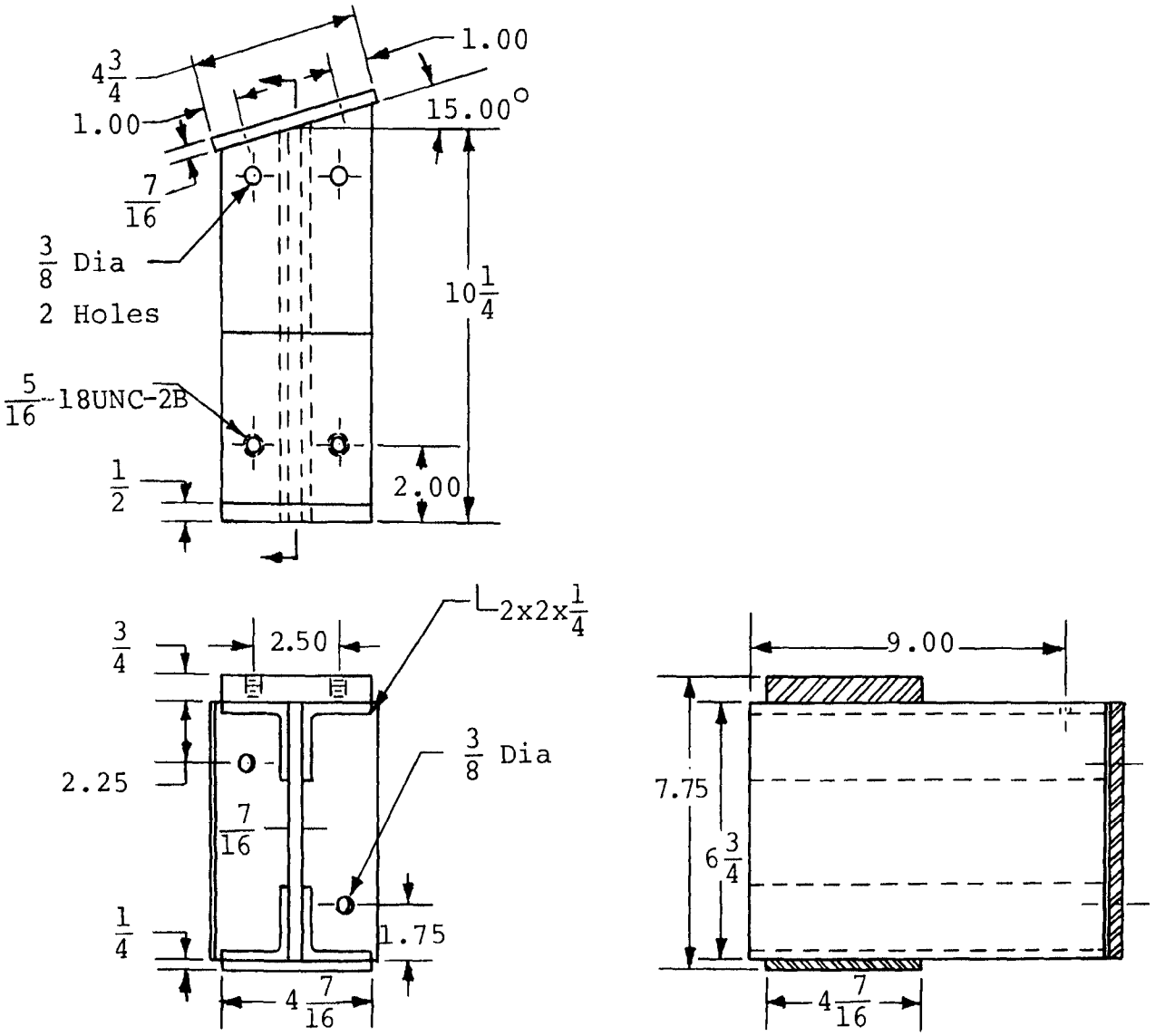

Fig. A.5 Machine Mounting

Scale- 1:5

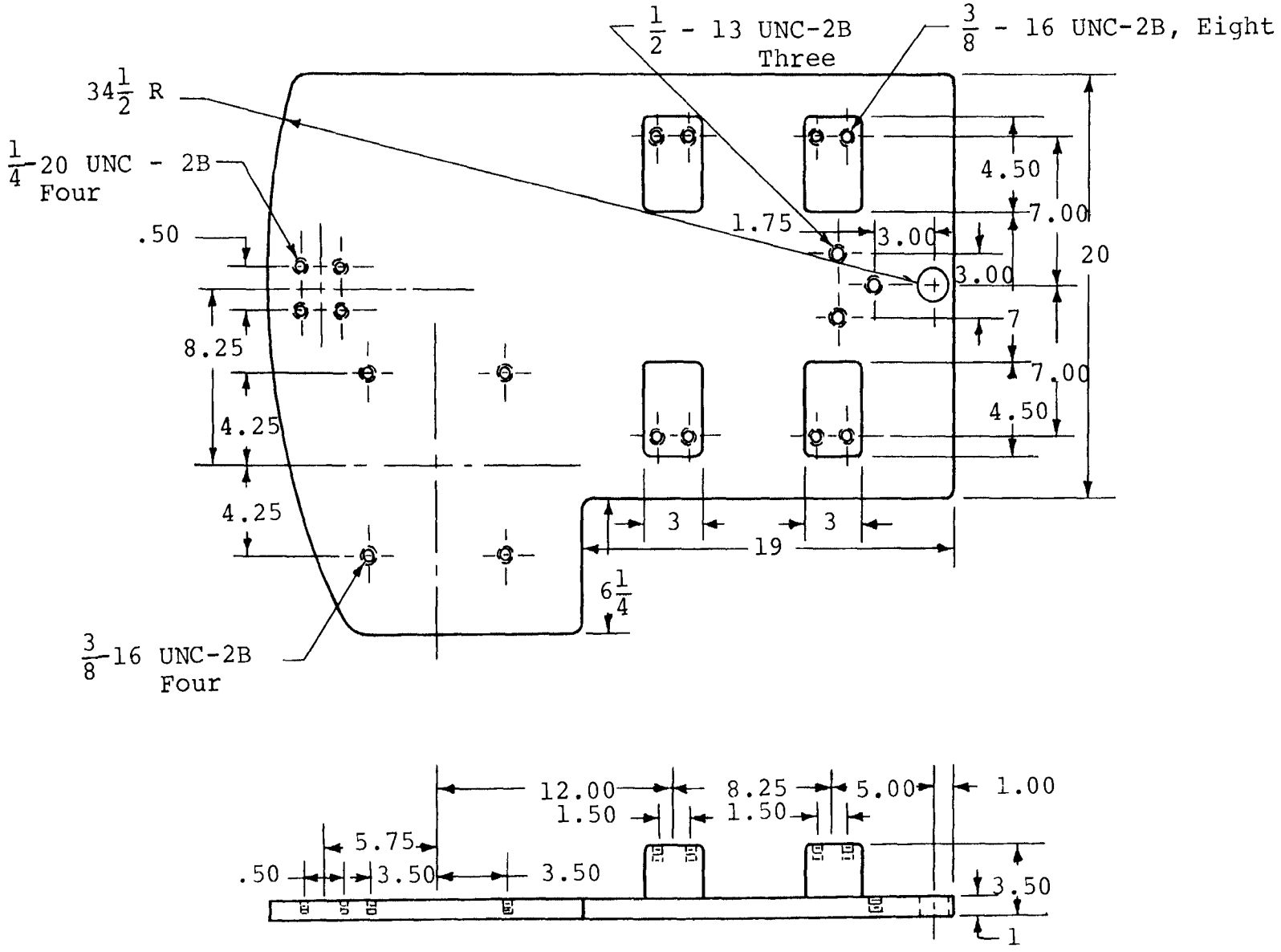

Material-steel

Fig. A.6 Drive Plate

Scale- 1:8

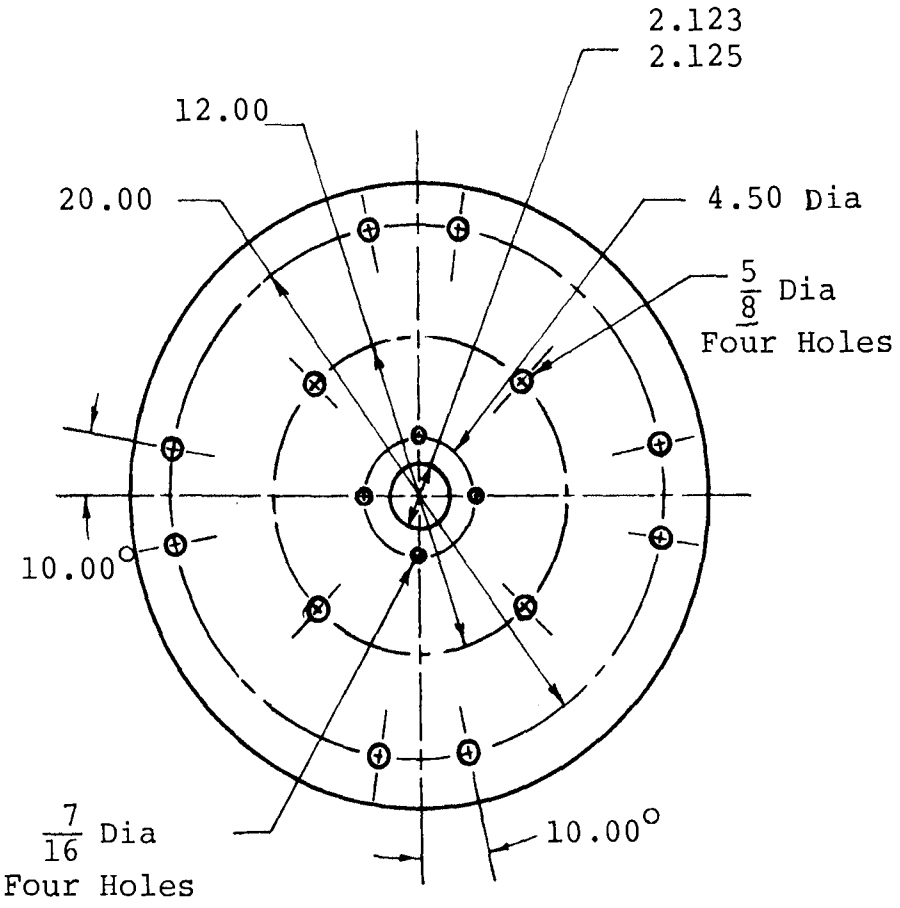

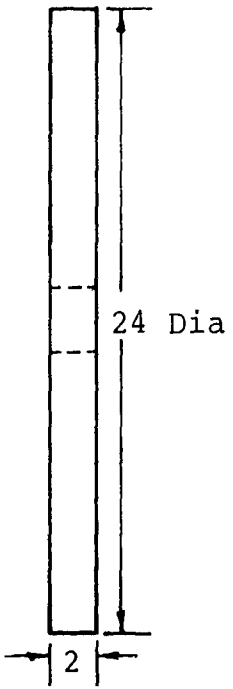

Material-Steel

Fig. A.7 Flywheel

Scale- 1:8

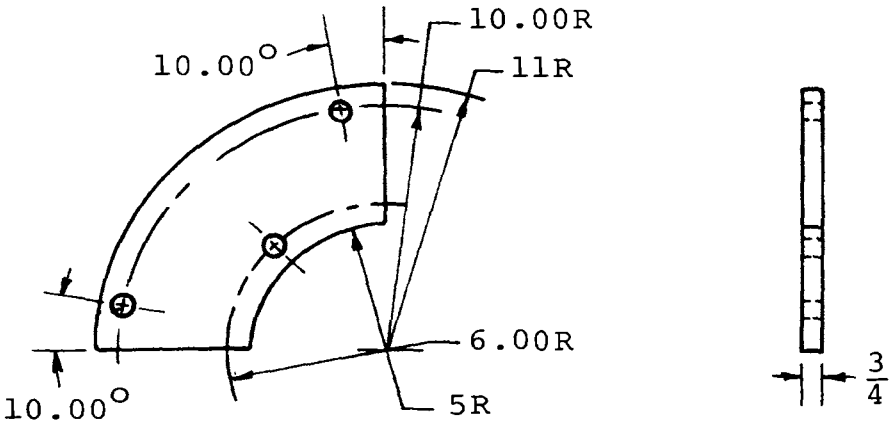

Material-Steel Fig. A.8 Flywheel Segment Scale-1:8

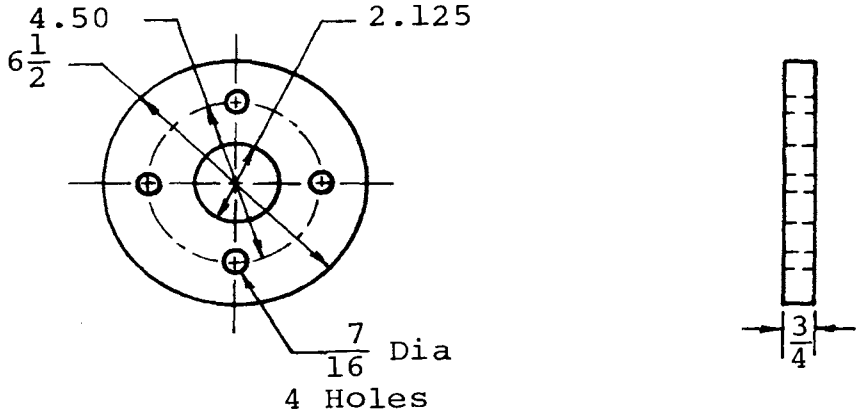

Material-Steel Fig. A.9 Flange Scale- 1:5

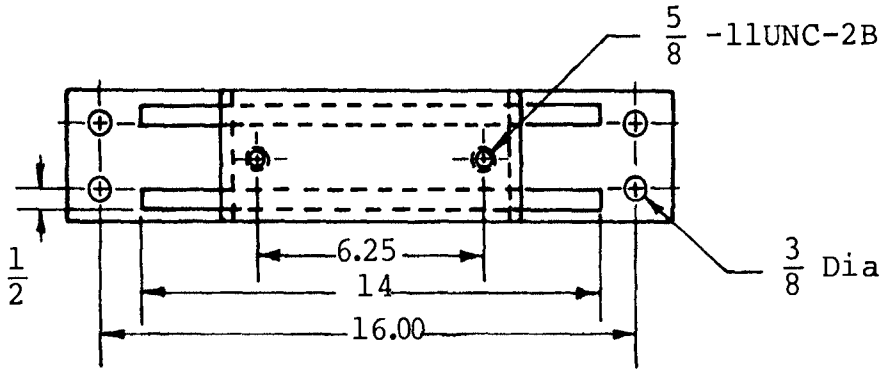

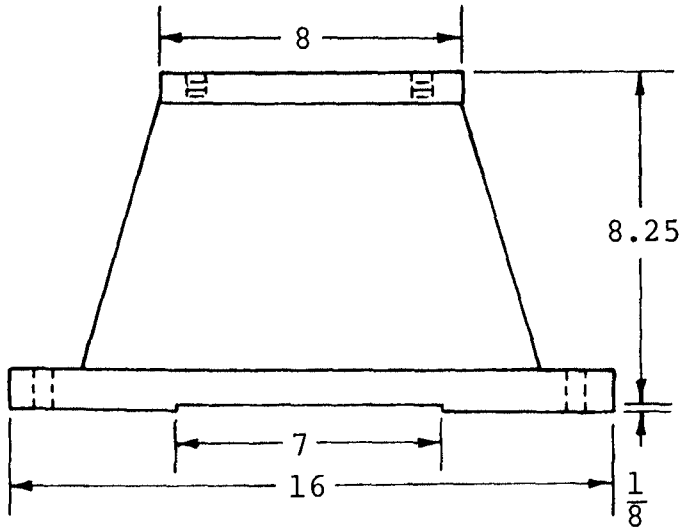

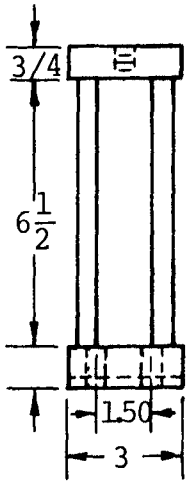

Material-Steel

Fig. A.10 Drive Shaft Bearing Support

Scale- 1:5

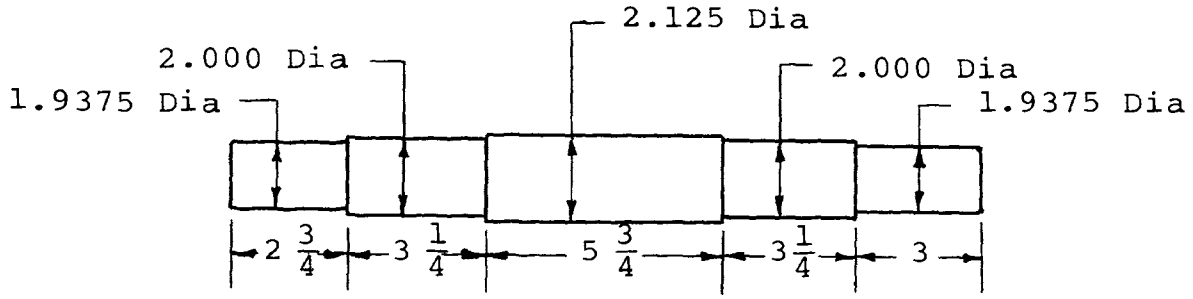

Material-Steel Fig. A.11. Drive Shaft Scale- 1:5

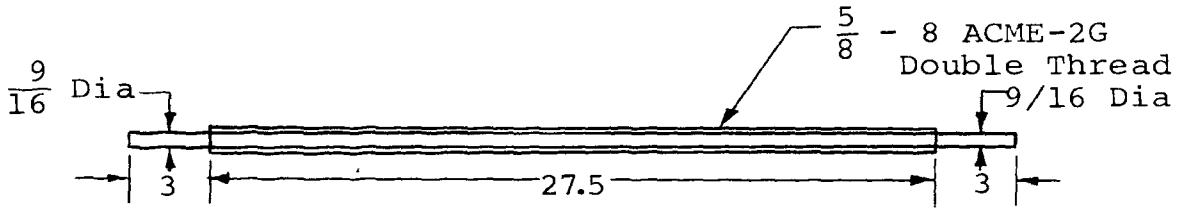

Fig. A.12. Adjusting Screw Scale - NTS

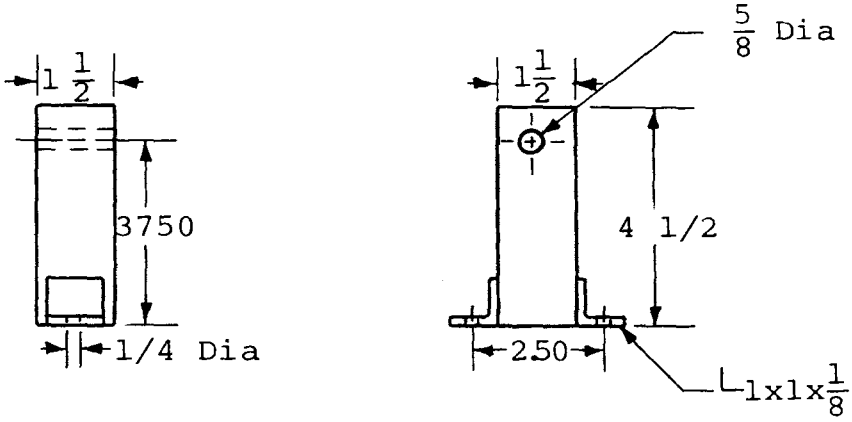

Material-Steel Fig. A.13. Screw Support Scale- 1:4

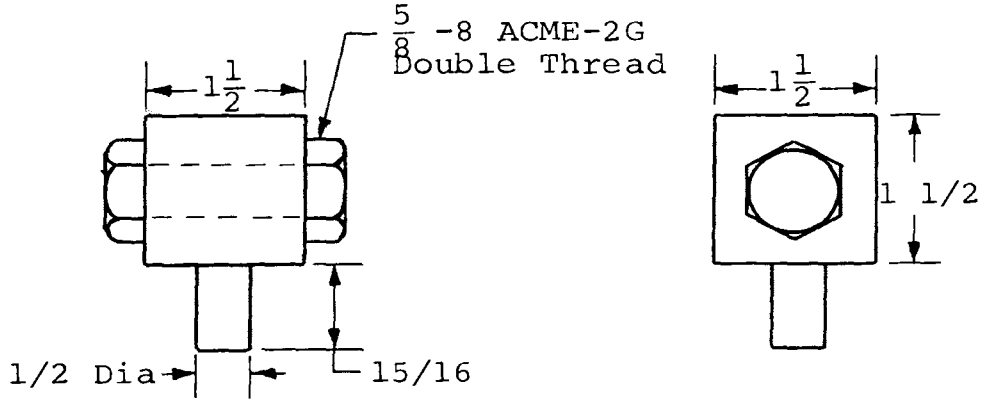

Material-Steel Fig. A.14. Nut Scale-1:2

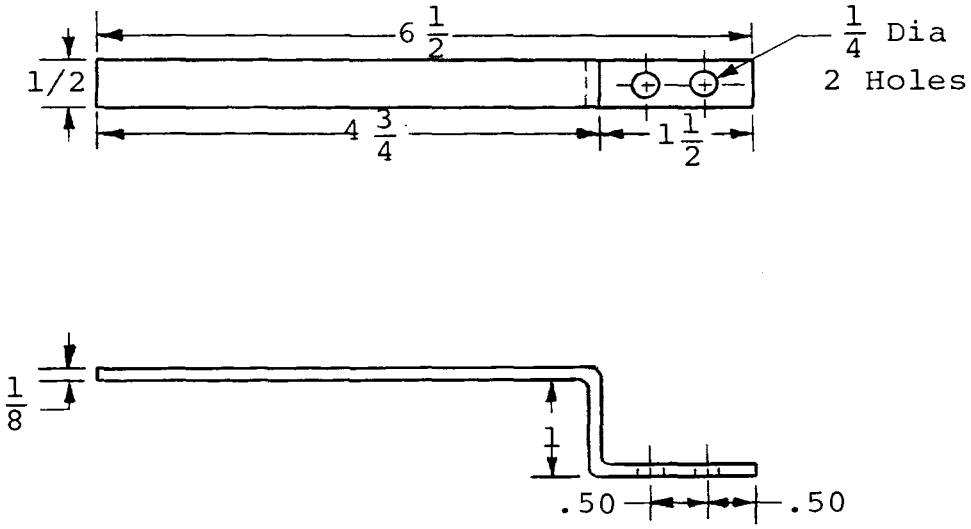

Material-Steel Fig. A.15 Guide Scale- 1:2

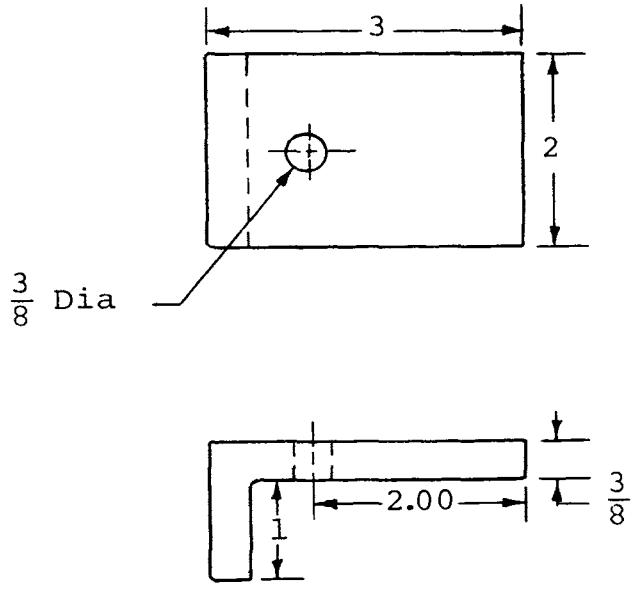

Material-Steel Fig. A.16 Locking Element Scale- 1:2

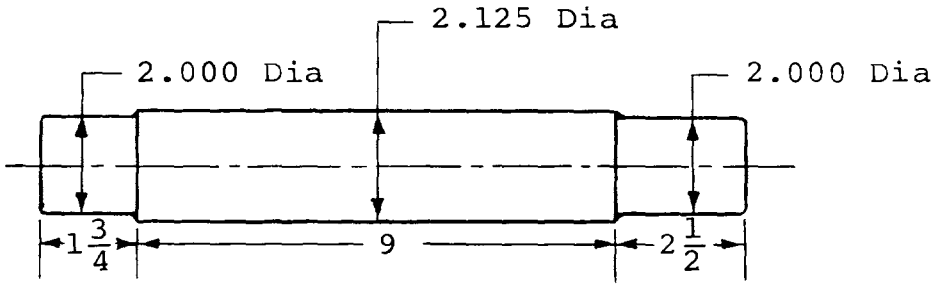

Material-Steel Fig. A.17 Driven Shaft Scale- 1:4

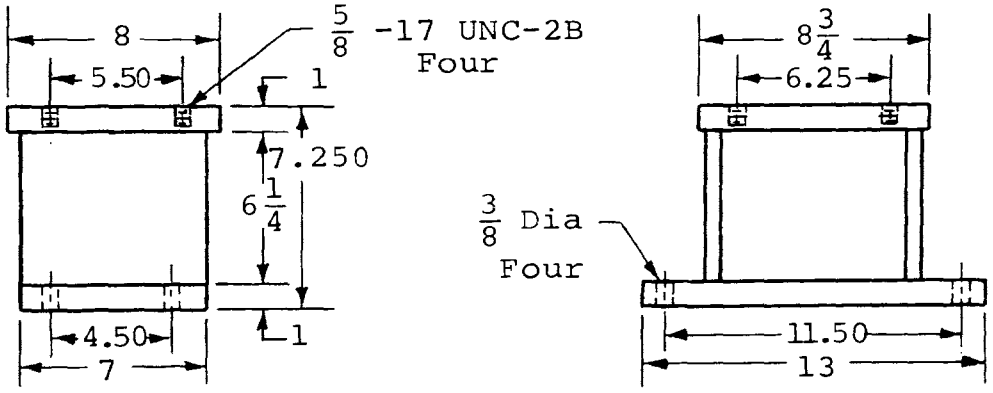

Material-Steel Fig. A.18 Driven Shaft Bearing Support Scale-1:8

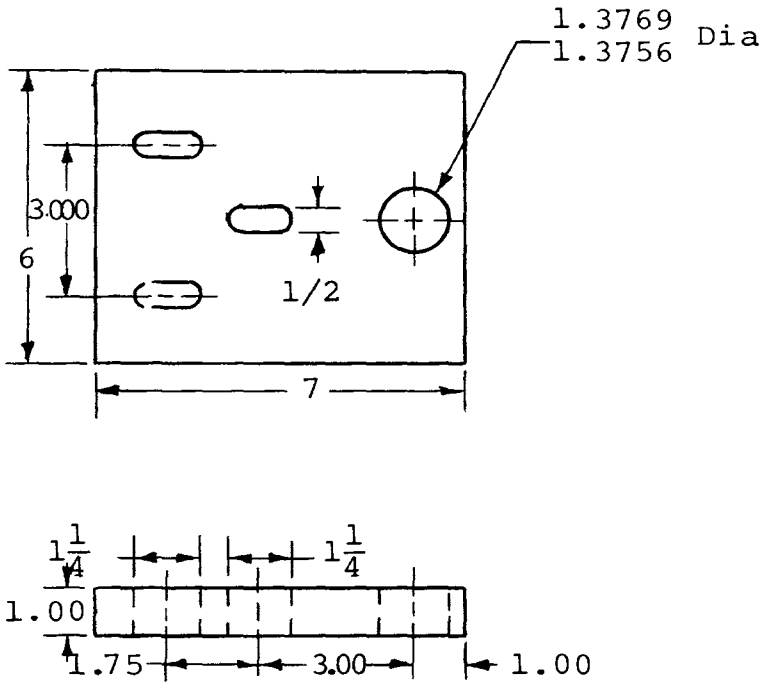

Material-Steel Fig. A.19 Pivot Plate 1 Scale- 1:4

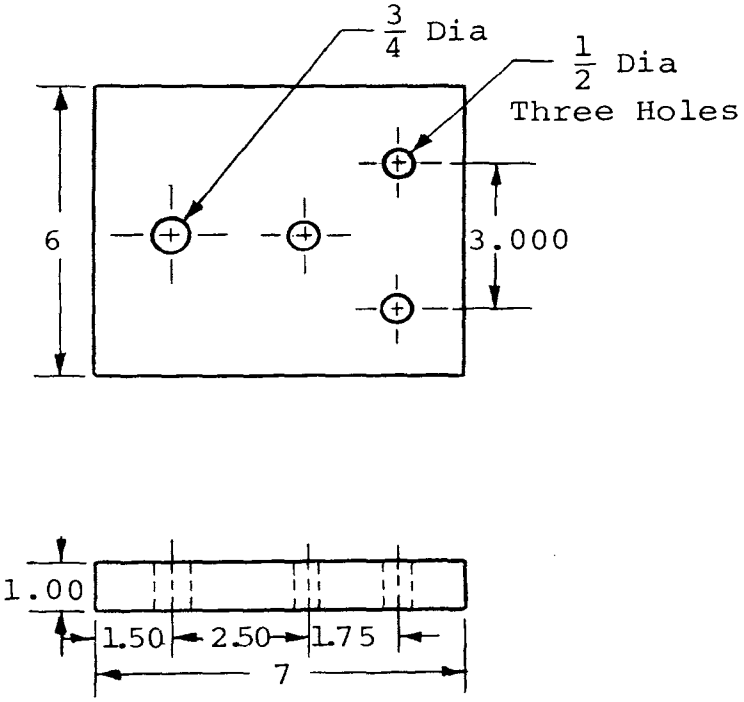

Material-Steel Fig. A.20 Pivot Plate 2 Scale- 1:4

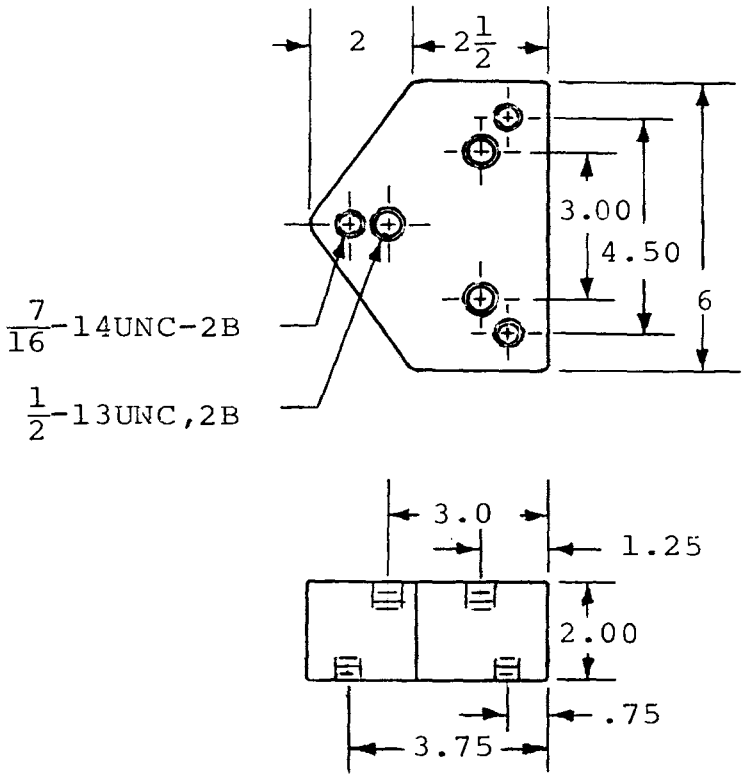

Material-Steel Fig. A.21 Pivot Block Scale- 1:6

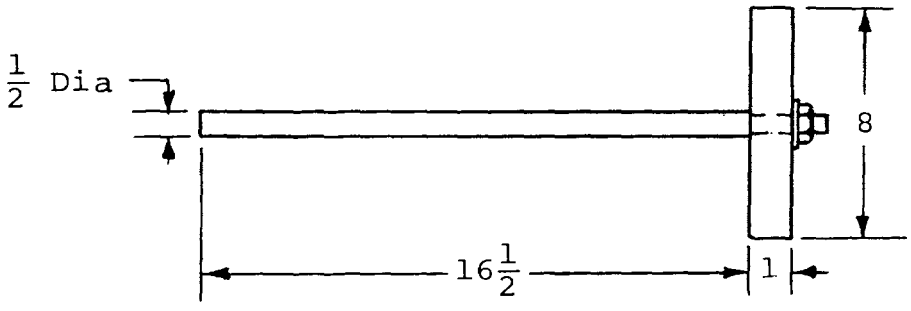

Fig. A.22 Specimen Scale-NTS

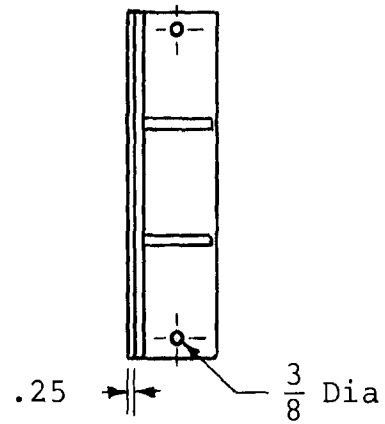

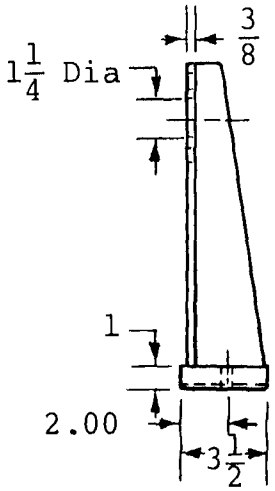

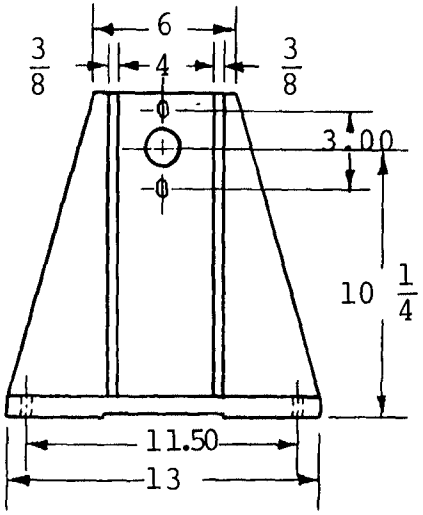

Material-Steel

Fig. A.23 Specimen Bearing Support

Scale- 1:8

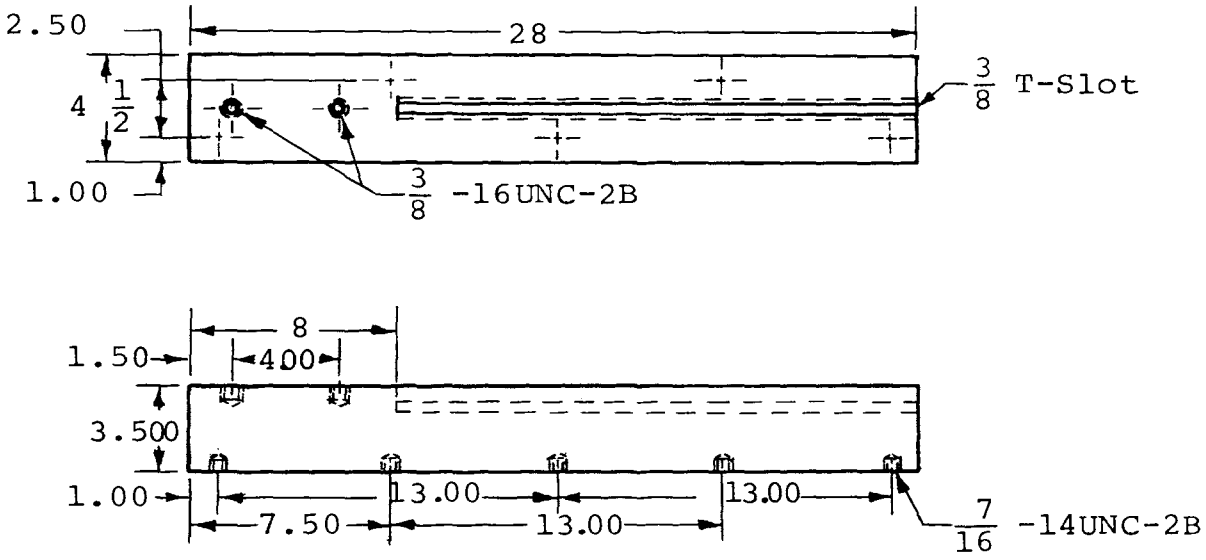

Fig. A.24 Steel Block 1 Scale 1:8

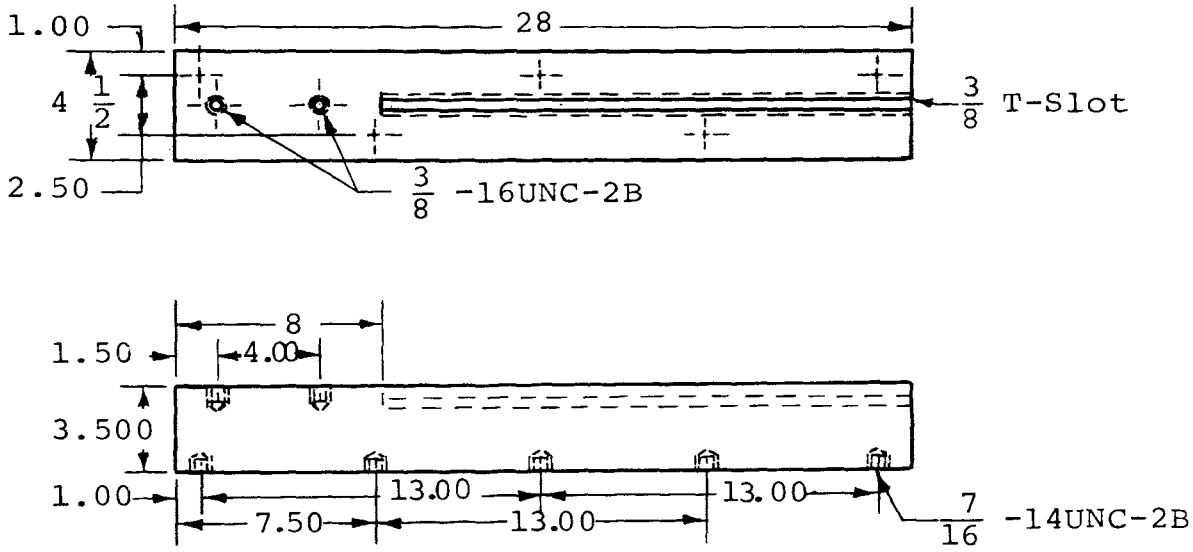

Fig. A.25 Steel Block 2 Scale- 1:8

Isomode Vibration Pads

Size - $4\frac{1}{2}$ x $4\frac{1}{2}$ x $\frac{5}{16}$

Number of Pads - 20

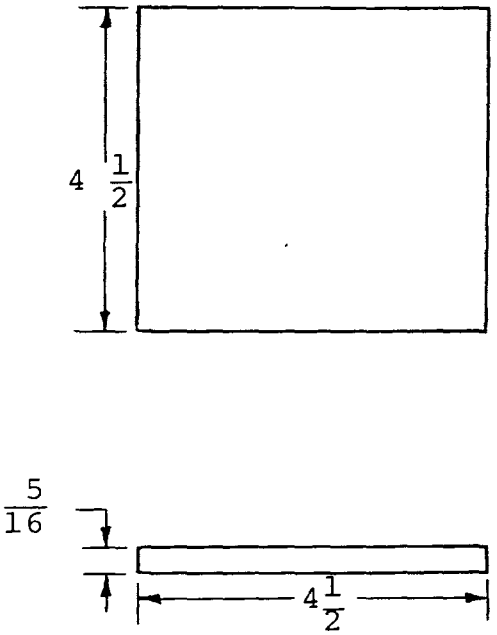

Material-Steel Fig. A.26 Pad-Plate Scale- NTS